

1 **Emission Factors and Optical Properties of Black and Brown Carbon Emitted at a Mixed-**
2 **Conifer Forest Prescribed Burn**

3
4 James D.A. Butler,^{1,2} Afsara Tasnia,³ Deep Sengupta,⁴ Nathan Kreisberg,⁵ Kelley C. Barsanti,^{3,6}
5 Allen H. Goldstein,^{1,5} Chelsea V. Preble,^{1,2} Rebecca A. Sugrue,^{1,2} Thomas W. Kirchstetter^{1,2,*}

6
7 ¹Department of Civil and Environmental Engineering, University of California, Berkeley,
8 Berkeley, California 94720

9
10 ²Energy Technologies Area, Lawrence Berkeley National Laboratory, Berkeley, California 94720

11
12 ³Department of Chemical and Environmental Engineering, Center for Environmental Research
13 and Technology, University of California, Riverside, Riverside, California 92507

14
15 ⁴Department of Environmental Science, Policy, and Management, University of California,
16 Berkeley, Berkeley, California 94720

17
18 ⁵Aerosol Dynamics Inc., Berkeley, California 94720

19
20 ⁶Atmospheric Chemistry Observations and Modeling, U.S. National Science Foundation
21 National Center for Atmospheric Research, Boulder, Colorado 80301

22
23 *Corresponding author email: twkirchstetter@lbl.gov

24 **Abstract**

25 Prescribed burning is a fuel management practice employed globally that emits carbonaceous

26 aerosols that affect human health and perturb the global climate system. Fuel-based Aerosol

27 black and brown carbon (BC and BrC) emission factors were calculated from ground and aloft

28 smoke during prescribed burns at a mixed-conifer, montane forest site in the Sierra Nevada in

29 California. BC emission factors were 0.52 ± 0.42 and $1.0 \pm 0.48 \text{ g kg}^{-1}$ for the smoldering and

30 flaming combustion phases. Modified combustion efficiency MCE is a poor predictor of BC

31 emission factor, in this study and published literature. We discuss limitations of using generalized

32 BC to $\text{PM}_{2.5}$ mass emission ratios to generate emissions inventories; u. Using BC emission

33 factors measured in this study, we recommend BC to $\text{PM}_{2.5}$ ratios of 0.7% and 9.5% for the

34 smoldering and flaming combustion in mixed-conifer prescribed burns. We apportioned the

35 measured aerosol spectral absorption between BrC and BC and calculated absorption Ångström

36 exponents (AAE) ~~based on multiwavelength absorption for BrC and BC of 6.26 and 0.67,~~

37 respectively. Using ~~Using~~ the Delta C method with a BrC-specific absorption cross-section, we

38 estimated BC concentrations and a smoldering combustion BrC emission factor of $7.0 \pm 2.7 \text{ g kg}^{-1}$,

39 nearly 14 and 7 times greater than the smoldering and flaming BC emission factors.

40 Furthermore, we estimate that BrC would account for 23% and 82%, respectively, of the solar

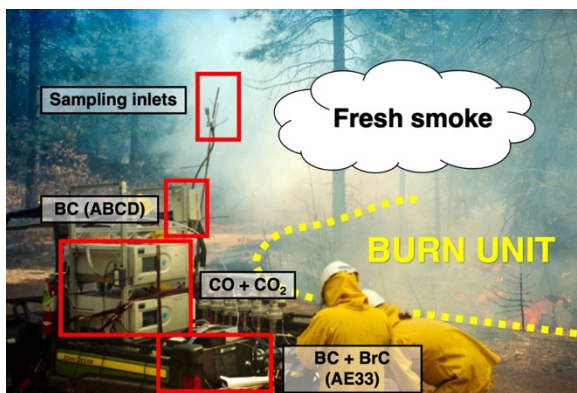
41 radiation absorbed by the smoldering smoke in the atmosphere integrated over the solar spectrum

42 (300–2500 nm) and in the UV spectrum (300–400 nm), indicating that BrC affects tropospheric

43 photochemistry in addition to atmospheric warming.

44

45 **Key Figure**



46

47

48 **Keywords**

49 Prescribed burn, black carbon, brown carbon, emission factor, light absorbing aerosol, wildland
50 fire fuel consumption model

51

52 **1 Introduction**

53 Prescribed burns are controlled burns that consume excess and dead fuel in an ecosystem,
54 like the duff, shrubs and dead biomass in the forest understory, or floor. In contrast, wildfires are
55 uncontrolled burns that may consume both the understory and overstory, or canopy, of a forest
56 and may spread to nearby property, endangering the homes and lives of people in the wildland
57 urban interface. Routine prescribed burns, or other fuel management practices like mechanical
58 thinning, reduce the risk and severity of wildfire ignition in forest ecosystems and increase the
59 resistance to ecosystem transition (i.e., conversion of forest to shrubland) caused by wildfires
60 (Steel et al., 2021; Wu et al., 2023).

61 Prescribed burns and wildfires emit fine particulate matter (PM_{2.5}), carbon monoxide
62 (CO), carbon dioxide (CO₂), volatile organic compounds, and nitrogen oxides (Andreae, 2019;
63 Urbanski, 2014; Urbanski et al., 2008; Wiedinmyer et al., 2006). Emitted PM_{2.5} includes organic
64 aerosol, some of which is light-absorbing brown carbon (BrC), and black carbon (BC). Whereas
65 BC absorbs solar radiation broadly across the visible spectrum, BrC light absorption is highly
66 wavelength dependent and strongest in the near-UV spectral region (Bond et al., 2004;
67 Kirchstetter et al., 2004; Laskin et al., 2015). Due to their perturbation of the radiative balance of
68 the atmosphere and short atmospheric residence time compared to CO₂, BC, and BrC are
69 considered short-lived climate forcers (Feng et al., 2013; Kirchstetter and Thatcher, 2012; Zhang
70 et al., 2020). Additionally, BC and BrC surface deposition in snowy climates reduces the solar
71 reflectance of snow and may accelerate snow melt (Chelluboyina et al., 2024; Hadley and
72 Kirchstetter, 2012; Kaspari et al., 2015; Yang et al., 2015). Human exposure to carbonaceous
73 aerosols also has detrimental health effects including cardiovascular disease, lung cancer,
74 adverse birth outcomes, and premature mortality (Dong et al., 2023; Grahame et al., 2014;
75 Janssen et al., 2011). Wildland fires are a major source of pollution relevant to human exposure
76 and account for one third of total PM_{2.5} emissions in the U.S., with roughly equal contributions
77 from prescribed burns and wildfires (Larkin et al., 2020).

78 Wildland fire modeling frameworks, or smoke models, estimate the amount of smoke
79 emitted during burn events to create input emissions necessary for climate modeling, air
80 pollution modeling, and health impact assessments (California Air Resources Board, 2020;
81 Connolly et al., 2024; Cruz Núñez et al., 2014; Maji et al., 2024). Smoke emissions from
82 wildland fires are estimated with fuel consumption models like Burnup, part of the First-Order
83 Fire Effects Model (FOFEM), and CONSUME, part of the BlueSky Smoke Modeling
84 Framework (Keane and Lutes, 2018; BlueSky Modeling Framework, 2024). Both smoke models
85 compute total emissions of a pollutant by multiplying pollutant emission factors by the mass of
86 fuel consumed during both the high intensity and low intensity stages of a burn event, which
87 roughly correspond to the flaming and smoldering phases of a wildland fire.

88 The differences in fuel mass consumption and temperature in these phases affect the
89 emission rate of pollutants, sometimes by an order of magnitude. In the flaming phase, fuel mass
90 consumption and temperature are highest and combustion is more complete, while both are lower
91 in the smoldering phase that is characterized by incomplete combustion (Urbanski, 2014).
92 Flaming combustion generally has a higher emission rate of BC and a lower emission rate of BrC
93 compared with smoldering combustion, while smoldering combustion is marked by higher
94 emissions of CO and BrC (Chen et al., 2007). Experiments designed to quantify pollutant
95 emissions must consider the placement of sampling instrumentation to capture these distinct
96 combustion phases of a burn, with aerial sampling platforms more likely to capture a mixture of
97 flaming and smoldering combustion due to the convective lofting of smoke caused by flaming
98 combustion (Aurell et al., 2021). Ground-level smoke, on the other hand, tends to be dominated
99 from smoldering combustion (Aurell and Gullett, 2013).

100 In this study, we conducted field sampling of pollutant emissions from prescribed burning
101 of a mixed-conifer understory and computed BC emission factors, BrC emission factors, and
102 aerosol absorption properties with ground and aerial sampling platforms. We investigate the
103 relationship between BC emission factors and combustion conditions and, finding that the
104 modified combustion efficiency (MCE) is a poor predictor of BC emission factor, propose a
105 framework to aggregate emission factors by either flaming or smoldering conditions to convey
106 the average value and variability of emission factors within these combustion regimes in fuel
107 consumption models. We report BC/PM_{2.5} ratios, or speciation profiles, for a mixed-conifer

108 understory prescribed burn. We then discuss how applying an incorrect BC/PM_{2.5} ratio in
109 wildland fire modeling frameworks may lead to large errors in BC emissions, using the
110 ecosystem studied in this work as an example. We compute the absorption Ångström exponent
111 (AAE) for the prescribed burn smoke aerosols, demonstrating that AAE is sensitive to the
112 wavelengths used in its calculation, and present estimates of AAE separately for BC and BrC to
113 estimate their contributions the solar radiation absorbed by the smoldering smoke in the
114 atmosphere.

115

116 **2 Materials and Methods**

117 **2.1 Field Measurements**

118 Field measurements were made at the Blodgett Forest Research Station (38.915224, -
119 120.662420), located 1370 meters above sea level on the western slope of the Sierra Nevada, 21
120 km east of Georgetown, CA. Prescribed burns were conducted in a mixed conifer forest, typical
121 of montane ecosystems of the Sierra Nevada (North et al., 2016). Three forest units were burned
122 in consecutive days in April 2021, as shown in Figure S1 in the Supporting Information (SI). The
123 prescribed burn on the first day escaped the designated unit (A) and the burn was terminated
124 early. The remainder of unit A was burned on the second day and units B and C were burned on
125 the third and fourth days, respectively.

126 Prescribed burn smoke was measured using both a ground and an aerial sampling
127 platform. The ground platform consisted of pollutant analyzers secured to a utility task vehicle
128 stationed immediately downwind of the fire to capture fresh smoke two meters above ground
129 level (see Figure S2). The ground platform was moved once each day as the burns progressed
130 and winds shifted to be on service roads nearby the highest intensity burn activity and the aerial
131 platform takeoff/landing location. Across the four days, there were nine ground sampling
132 sessions: at two locations on each day, plus one “next-day” smoldering sample on the second day
133 for burn unit A before ignition of the remaining unit. For the aerial platform, pollutant analyzers
134 were attached to the unmanned aerial vehicle, a DJI Matrice 600 Pro hexacopter. Concurrent
135 with ground sampling, the unmanned aerial vehicle was flown 23 times across the four days with
136 at least five flights each day and a maximum of 10 flights on the third day. [The aerial platform](#)
137 [was flown in the densest smoke plumes to intercept the bulk of the prescribed burn smoke and](#)

138 [hovered within these plumes to capture fresh emissions representative of the event.](#) The average
139 elevation of aerial platform throughout sampling was 29 meters, with an average sampling
140 elevation range of 16–42 meters across all flights.

141 BC, CO, and CO₂ were measured on both the ground and aerial sampling platforms. BC
142 was measured using two filter-based aerosol absorption photometers: the Aerosol Magee
143 Scientific aethalometer model AE33 with a 2.5 μm cyclone on the inlet on the ground platform
144 and the custom-built Aerosol Black Carbon Detector (ABCD) on both the ground and aerial
145 platforms (Caubel et al., 2018; Sugrue et al., 2024). [These instruments estimate BC](#)
146 [concentrations from measured aerosol light absorption and wavelength-specific absorption cross](#)
147 [section.](#) The ABCD estimates BC concentration based on aerosol optical attenuation at 880 nm
148 wavelength (λ). The AE33 also measures BC at $\lambda=880$ nm, in addition to aerosol optical
149 attenuation at six other wavelengths. In particular, the AE33 reports the mass concentration UV-
150 absorbing aerosol (UVPM) based on the optical attenuation at 370 nm. BrC concentration was
151 estimated from these data as described below in Section 2.2. [Filter-based aerosol absorption](#)
152 [photometry has well known limitations due to the interactions of the collected aerosol particles](#)
153 [and filter media. Corrections for these sampling artifacts are detailed in the Supporting](#)
154 [Information, SI.](#)

155 Collocating the AE33 with the ABCD on the ground enabled an analysis to express BC
156 measured with the ABCD in terms of AE33 equivalence, also described below. CO and CO₂
157 were measured by non-dispersive infrared (NDIR) absorption photometry on the ground
158 platform using Horiba models APMA370 and APCA370, respectively. ([Tasnja et al.,](#)
159 [2025](#)) ([Tasnja et al., n.d.](#)) CO and CO₂ were measured on the aerial platform with an
160 electrochemical cell (Alphasense CO-B4) and NDIR sensor (PP Systems SBA-5), respectively.
161 All instruments reported pollutant concentrations at 1 Hz frequency. Data were post-processed
162 and validated prior to analysis using the quality assurance and control measures described in the
163 SI, including pollutant concentration time-series alignment and loading artifact correction of BC
164 concentrations measured with the ABCD.

165

166 **2.2 Calculations**

167 Light absorption by carbonaceous aerosols increases with decreasing wavelength, a trend
168 that is often modeled as a power-law:

169 $b_{abs}(\lambda) \propto \lambda^{-AAE}$ (Equation 1)

170 AAE was calculated by an ordinary least squares linear regression of the natural log
171 transformation of λ and $b_{abs}(\lambda)$. Here, $b_{abs}(\lambda)$ (m^{-1}) was calculated by multiplying the
172 wavelength-dependent, loading artifact-corrected, light-absorbing aerosol concentration reported
173 by the AE33 by the wavelength-dependent mass absorption cross-section of BC on a filter (m^2
174 g^{-1}). Aerosol absorption was calculated per second and then averaged per minute with a 90% data
175 completeness threshold applied at seven wavelengths measured by the ground aethalometer.

176 The Delta-C method has been used to estimate BrC concentrations with a multi-
177 wavelength aethalometer (Harrison et al., 2013; Huang et al., 2011; Stampfer et al., 2020;
178 Wagstaff et al., 2022; Wang et al., 2010, 2011a, b), where BrC is the difference between UVPM
179 and BC concentrations in units of $\mu g m^{-3}$. BrC mass concentrations were calculated using the
180 Delta-C method, which estimates BrC as the difference between UVPM and BC concentrations
181 in units of ($\mu g m^{-3}$):

182 $BrC = UVPM - BC$ (Equation 2)

183 The AE33 aethalometer assumes light absorption at 880 nm is entirely due to BC and For the
184 variables in Equation (2), UVPM is the mass concentration of all light absorbing aerosol at
185 reported at 370 nm. The AE33 further assumes that UVPM has the same absorption cross-section
186 as BC (i.e., 18.47 $m^2 g^{-1}$ at 370 nm). Thus, a direct application of Equation 2 implicitly assumes
187 that BrC has the same absorption cross-section as BC. and BC is the mass concentration
188 reported at 880 nm

189 In this study, we improve upon this method to estimate BrC concentrations. We first
190 determine the contribution of BrC to total aerosol absorption at 370nm:

191 $b_{abs,BrC}(370nm) = b_{abs}(370nm) - b_{abs,BC}(370nm)$ (Equation 3)

192 We estimate BC absorption at 370 nm, $b_{abs,BC}(370nm)$, by extrapolating the . The Delta-C method
193 is established in literature as the approach to estimate BrC concentrations with an aethalometer in
194 real time (Harrison et al., 2013; Huang et al., 2011; Stampfer et al., 2020; Wagstaff et al., 2022;
195 Wang et al., 2010, 2011a, b). As described above, the AE33 as often applied in prior studies,
196 measured aerosol light absorption at 880 assuming $AAE_{BC} = 0.67$. Whereas $AAE_{BC} = 1$ is a

197 commonly used value that is consistent with Mie theory (i.e., uncoated, ideal spherical particles
 198 with wavelength-independent refractive index) (Liu et al., 2018), the value 0.67 was estimated
 199 based on the optical properties of the smoke measured in this study, as described below in
 200 Section 3.3. We then calculate projects BC absorption across its measured wavelengths to the
 201 near UV wavelengths assuming $\text{AAE}_{\text{BC}} = 1$. The Delta C method and attributes excess light-
 202 absorption to BrC, where UVPM and, thus BrC, are assumed to have the same absorption cross-
 203 section as BC ($18.47 \text{ m}^2 \text{ g}^{-1}$ at 370 nm) (Harrison et al., 2013; Huang et al., 2011; Stampfer et al.,
 204 2020; Wagstaff et al., 2022; Wang et al., 2010, 2011a, b). BrC concentration is thus operationally
 205 defined rather than an actual mass concentration. In this study, we improve upon the Delta C
 206 method as previously implemented with the AE33 by using a BrC concentration by dividing
 207 $b_{\text{abs,BrC}}(370\text{nm})$ by the current best estimate of the BrC mass absorption cross-section empirically
 208 determined by Ivančić et al. ($4.5 \text{ m}^2 \text{ g}^{-1}$ at 370 nm) rather than assuming BrC and BC have the
 209 same absorption cross-section and estimate the contribution of BC to each sample's spectral
 210 attenuation, $b_{\text{abs,BC}}(\lambda)$, by attributing all attenuation at 880 nm to BC and extrapolating to other
 211 wavelengths assuming $\text{AAE}_{\text{BC}} = 0.67$. This is the AAE_{BC} value determined in this study, as
 212 described below in Section 3.3. In doing so, our BrC concentrations are equivalent to those
 213 reported by the newest model of the aethalometer (i.e., the AE36) (Aerosol d.o.o., 2024).

214 Following the approach presented in Kirchstetter and Thatcher (2012), we computed the
 215 contribution of BrC to smoldering smoke aerosol absorption of solar radiation. The contribution
 216 of BrC to spectral absorption in each smoke sample, $b_{\text{abs,BrC}}(\lambda)$, is determined by subtracting the
 217 BC absorption from the total absorption with:

$$b_{\text{abs,BrC}}(\lambda) = b_{\text{abs}}(\lambda) - b_{\text{abs,BC}}(\lambda) \quad (\text{Equation 3})$$

218 Based on the apportionment of spectral absorption to BC and BrC, we compute the fraction
 219 of spectral radiation for smoldering smoke at each wavelength in the solar spectrum that would
 220 be absorbed by BrC:

$$f_{\text{BrC}} = \frac{b_{\text{abs,BrC}}(\lambda)}{b_{\text{abs}}(\lambda)} \quad (\text{Equation 4})$$

221 Last, we compute the fraction of solar radiation that BrC in the smoldering smoke would absorb
 222 in the atmosphere:

$$F_{\text{BrC}} = \frac{\int_{\lambda_1}^{\lambda_2} f_{\text{BrC}}(\lambda) \cdot i(\lambda) d\lambda}{\int_{\lambda_1}^{\lambda_2} i(\lambda) d\lambda} \quad (\text{Equation 5})$$

226 where $i(\lambda)$ is the clear sky air mass one global horizontal solar spectrum at the earth's surface
227 (Levinson et al., 2010). We evaluate F_{BrC} using two sets of integration bounds (λ_1, λ_2) : (1) across
228 the full solar irradiance spectrum from 300 to 2500 nm that is meaningful for atmospheric
229 warming and (2) in the near-UV from 300 to 400 nm that is more relevant to tropospheric
230 photochemistry (Li and Li, 2023; Mok et al., 2016).

231 The modified combustion efficiency (MCE) is typically used to assess the combustion
232 completeness during biomass burning and was calculated as the mass fraction of fuel C emitted
233 as CO_2 compared to CO_2 and CO (Ward and Radke, 1993):

234
$$MCE = \frac{\Delta CO_2}{\Delta CO_2 + \Delta CO} \quad (\text{Equation 6})$$

235 Background-subtracted concentrations ΔCO and ΔCO_2 were calculated as the difference between
236 measured concentrations and background concentrations, [the latter of which were established](#)
237 [separately for each of the four days of sampling as described in the SI \(listed in Table S2\).](#) MCE
238 is unitless, and a value of 0.9 is commonly used as a threshold to distinguish between flaming-
239 dominated ($MCE > 0.9$) and smoldering-dominated ($MCE < 0.9$) combustion (Selimovic et al.,
240 2018).

241 Fuel-based BC and BrC emission factors (EF_i) in units of grams BC and BrC emitted per
242 kilogram fuel consumed ($g \text{ kg}^{-1}$) were calculated by the carbon balance method: [Nelson Jr.,](#)
243 [1982](#)

244
$$EF_i = \frac{w_c * V_m}{MW_c} \int_{t_0}^{t_1} \frac{\Delta C_i}{(\Delta CO + \Delta CO_2)} dt \quad (\text{Equation 7})$$

245 where ΔC_i is the background-subtracted BC or BrC concentration ($\mu\text{g m}^{-3}$), $w_c = 0.5$ is the weight
246 fraction of carbon in [conifer forest fuels \(Thomas and Martin, 2012\)](#), [the biomass fuel \(Urbanski,](#)
247 [2014\)](#), V_m is the molar volume of air and equal to $0.024 \text{ m}^3 \text{ mol}^{-1}$, MW_c is the molar mass of
248 carbon and equal to 12 g mol^{-1} , and ΔCO and ΔCO_2 are mixing ratios (ppm) [\(Akagi et al., 2011\)](#).
249 [In Equation \(7\), the carbon balance method assumes that all fuel carbon is emitted as either CO](#)
250 [or \$CO_2\$, given 90–98% of total emitted carbon is emitted as these gases \(Akagi et al., 2011; Binte](#)
251 [Shahid et al., 2024; Nelson Jr., 1982; Yokelson et al., 2013\)](#). Emission factors were calculated by
252 integration of the background-subtracted pollutant concentrations over different time intervals.
253 The integration bounds for the aerial emission factors were the start and end times of each flight,
254 with a temporal basis equal to the total flight duration, or $t_1 - t_0$ in Eq. 4. Flight durations ranged

255 from 4–22 minutes. For the ground emission factors, the start time (t_0) was when the
256 aethalometer began collecting samples on a new filter spot and the attenuation (ATN) was zero.
257 The end time (t_1) was when the filter became saturated at an ATN ~~ofreached~~ 100. At that point,
258 the aethalometer advanced its filter tape. These integration bounds resulted in a ground sample
259 temporal basis that corresponded to the ATN cycle of the aethalometer, which ranged from 2–36
260 minutes. A detailed discussion of the [representativeness and](#) chosen temporal basis of the
261 emission factors is provided in the SI.

262

263 **3 Results and Discussion**

264 **3.1 Emission Factors**

265 BC and BrC emission factors measured on the ground and aloft are presented in Table 1.
266 Overall, the aerial platform measured smoke characterized by a higher modified combustion
267 efficiency ($MCE_{aerial} = 0.88 \pm 0.05$, average \pm standard deviation) and nearly 2 times higher BC
268 emission factor ($EF_{BC,aerial} = 0.92 \pm 0.48 \text{ g kg}^{-1}$) than the smoke measured on the ground
269 ($MCE_{ground} = 0.83 \pm 0.03$; $EF_{BC,ground} = 0.47 \pm 0.40 \text{ g kg}^{-1}$).

270

271 Table 1: Summary Statistics of Carbonaceous Aerosol Emission Factors and MCE (average \pm
272 standard deviation)

	Number of Samples	MCE	BC (g kg^{-1})	BrC (g kg^{-1})
Aerial samples	23	0.88 ± 0.05	0.92 ± 0.48	–
Ground samples	66	0.83 ± 0.03	0.47 ± 0.40	7.0 ± 2.7
Smoldering samples	77	<0.9	0.52 ± 0.42	–
Flaming samples	12	>0.9	1.0 ± 0.48	–
All samples	89	0.84 ± 0.04	0.59 ± 0.68	–

273

274 BC emission factors are plotted against MCE in Figure 1. Individual ground platform
275 samples are plotted as orange circles and aerial samples are plotted as blue squares. Nearly all
276 the smoke samples collected from the ground platform (64 of 66 ATN cycles) were associated
277 with smoldering combustion ($MCE < 0.9$). A roughly equal number smoke samples collected
278 aloft were associated with flaming-dominant combustion (10 flights) and smoldering-dominant
279 combustion (13 flights). BC emission factors demonstrated a weak positive linear correlation

(solid black line, $r^2 = 0.11$) against MCE values, with BC emission factors spanning an order of magnitude (0.11 to 1.70 g kg⁻¹) and MCE values ranging from 0.76 to 0.96. This relationship is similar to the weak positive linear trend reported by McMeeking et al. (2009) for a laboratory study ($r^2 = 0.09$), shown as a dashed black line in Figure 1a. In contrast, another laboratory study by Hosseini et al. (2013) reported a weak negative linear trend (dotted black line, $r^2 = 0.10$). The application of linear regression models to emission factor data would allow these field and laboratory studies to be scaled in fuel consumption models as a function of combustion conditions and/or fire intensity (Burling et al., 2011; May et al., 2014; Ottmar, 2014; Selimovic et al., 2018; Urbanski, 2014). However, given the very low coefficients of determination from this work and previous laboratory studies ($r^2 < 0.15$), MCE is not a strong predictor of the BC emission factor for smoke model estimates.

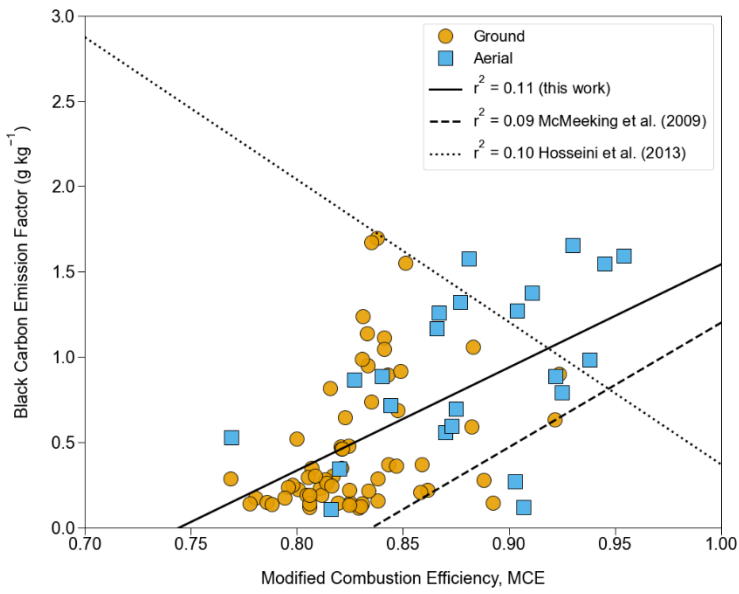
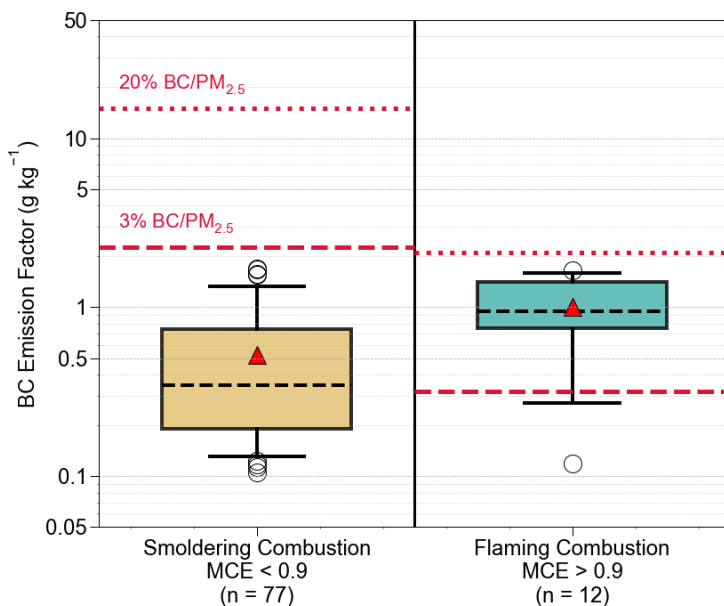


Figure 1: BC emission factors plotted against modified combustion efficiency for all samples. Symbology designates the ground (circles) and aerial (squares) measurement platforms. All samples fit with a linear regression model and compared to previous laboratory linear models of BC emission factors as a function of MCE (Hosseini et al., 2013; McMeeking et al., 2009).

3.2 Emissions Modeling in Fuel Consumption Models

BC emission factor distributions for flaming (MCE>0.9) and smoldering (MCE<0.9) conditions are presented in Figure 2. These combustion categories were chosen to match how smoke models calculate emissions, often with combustion-phase dependent emission factors.

301 Fuel consumption models (e.g., Burnup, CONSUME) compute the total fuel consumed
 302 separately during flaming and smoldering combustion phases of a burn. Smoke models then
 303 apply the appropriate EFs, with either one EF for flaming combustion and one EF for smoldering
 304 combustion (e.g., FOFEM), or using a linear model like [that](#) presented in Figure 1a [wherein](#)
 305 [which](#) the calculated MCE in the fuel consumption model is used to obtain the corresponding EF.
 306 The average BC emission factors measured during flaming combustion conditions in this study
 307 were nearly 2 times greater than those measured during smoldering conditions: $EF_{BC, \text{flaming}} = 1.0$
 308 $\pm 0.48 \text{ g kg}^{-1}$ versus $EF_{BC, \text{smoldering}} = 0.52 \pm 0.42$, with similar magnitude [as](#) the average
 309 emissions factors for aerial and ground samples reported above.
 310



311
 312 Figure 2: BC emission factors categorized into smoldering combustion ($MCE < 0.9$) and flaming
 313 combustion ($MCE > 0.9$) phases for input into fuel consumption. Boxes represent the
 314 interquartile range and tails the 5th and 95th percentile. The median is provided as the black
 315 dashed line across the box, the average as a red triangle, and outliers as open circles. Speciation
 316 profile-derived BC emission factors for 3% and 20% BC/PM_{2.5} for each combustion phase are
 317 plotted as red horizontal dashed and dotted lines, respectively. Note the logarithmic scale on the
 318 y-axis.
 319

320 Also included in Figure 2 are BC emission factors calculated with the FOFEM
 321 methodology as a fraction of PM_{2.5} emission factors from Burling et al. (2011) for a mixed-

322 conifer understory prescribed burn (Burling et al., 2011; Lutes, 2020). These BC emission factors
323 are plotted as horizontal lines across each combustion regime in Figure 2 and represent values
324 assumed in the most recent federal and California BC inventories. The 2020 National Emissions
325 Inventory (dashed line) assumes a 3% BC/PM_{2.5} mass ratio for all wildland fire sources,
326 including prescribed burns and wildfires (US Environmental Protection Agency, 2023). The 2013
327 California BC Emissions Inventory (dotted line) assumes a 20% BC/PM_{2.5} mass ratio for
328 prescribed burns (California Air Resources Board, 2016). These BC/PM_{2.5} mass ratios—or BC
329 speciation profiles—are known to be highly uncertain (Chow et al., 2011). For example, in the
330 EPA SPECIATE v5.3 database, prescribed burn BC/PM_{2.5} mass ratios vary from 3–11% and for
331 uncontrolled forest fire or forest fuel types between 0.8–80% (SPECIATE, 2025).

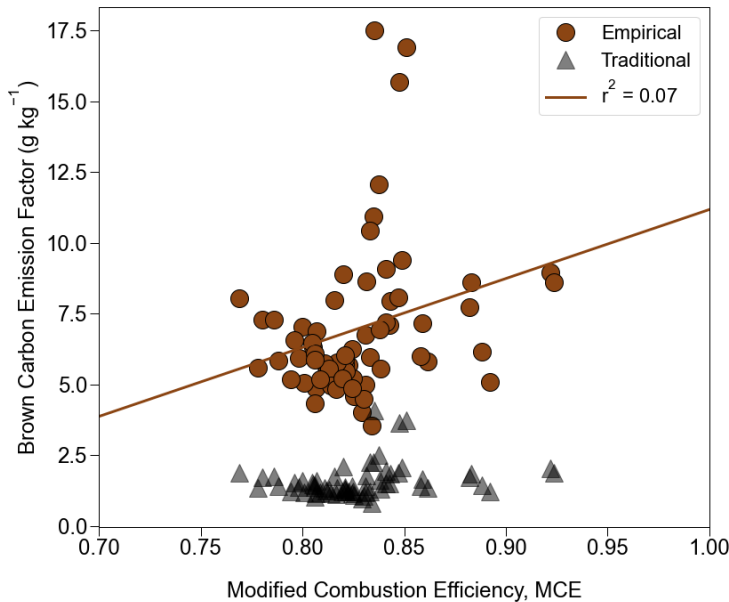
332 The difference between the average flaming and smoldering BC emission factors
333 measured in this study and the BC emission factors estimated from BC/PM_{2.5} ratios reveals the
334 current limitation in using the latter methodology in wildland fire modeling frameworks to
335 estimate BC emissions. PM_{2.5} emission rates for mixed-conifer forests and many other
336 ecosystems are higher under smoldering combustion than under flaming combustion, the
337 opposite of BC emission rates (Burling et al., 2011; Chen et al., 2007). As a result, BC emission
338 rates are erroneously predicted to be greater under smoldering combustion. The speciation
339 profiles assumed in the federal and California inventories overestimate BC emission factors
340 under smoldering combustion for this type of burn by a factor 4 and 29, respectively. Under
341 flaming combustion, the California inventory overestimates BC emission rates by a factor of 2,
342 whereas the federal inventory underestimates by 0.3. Dividing the average field BC emission
343 factors in this study by the literature PM_{2.5} emission factor [from Burling et al. \(2011\)](#) indicates
344 that a more appropriate BC speciation profile for a mixed-conifer understory prescribed burn
345 would be 0.7% and 9.5% for the smoldering and flaming combustion phases, respectively.

347 **3.3 Optical Properties and Apportionment of Aerosol Solar Radiation Absorption**

348 BrC emission factors were computed based on ground-level smoke measurements with
349 the multiwavelength aethalometer, most of which (64 of 66 samples) were during smoldering-
350 dominated combustion. There was a very weak positive linear relationship ($r^2 = 0.06$) between BrC
351 emission factors and MCE (Figure 3). The study average BrC emission factor was 7.0 ± 2.7 g

352 kg^{-1} . It is worth noting that this BrC emission factor, computed as described in Section 2.2 based
353 on an absorption cross-section specific to BrC, is 4.4 times greater than the emission factor
354 calculated using the more traditional Delta-C method, where the absorption-cross section of BrC
355 is operationally defined as equal to the absorption cross-section of BC.

356



357

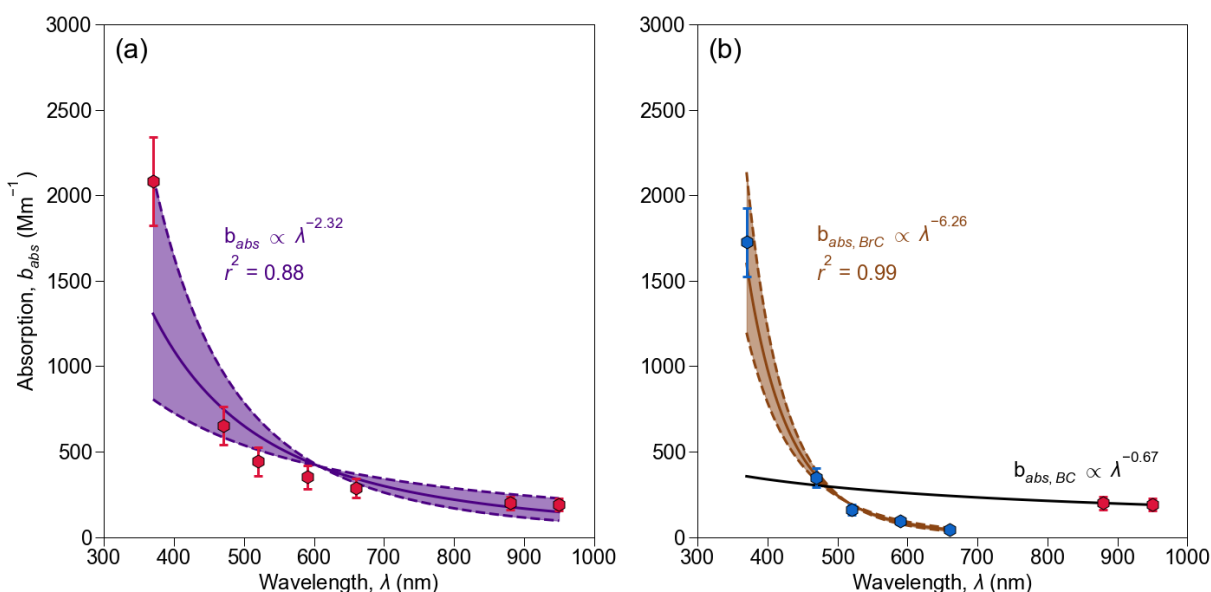
358 Figure 3: Ground BrC emission factors computed using the Delta-C method with a BrC-specific
359 mass absorption cross-section (denoted as Empirical and shown with brown circles) and the
360 more traditional approach using an operationally defined BrC mass absorption cross-section
361 equal to that of BC (denoted as Traditional and shown with grey triangles) plotted against
362 modified combustion efficiency. The solid brown line shows the linear regression for the BrC
363 emission factors calculated with the empirical approach.

364

365 Study-average spectral absorption curves are plotted in Figure 4. A power-law fit to the
366 data over all aethalometer wavelengths from 370–950 nm is shown in Figure 4a. The absorption
367 data are fit with two trend lines in Figure 4b: an extrapolation of the power law fit to the near-IR
368 data at 880 and 950 nm to illustrate the BC contribution to total absorption, $b_{\text{abs,BC}}(\lambda)$, and a
369 power law fit of the BrC contribution to absorption, $b_{\text{abs,BrC}}(\lambda)$, which extends from mid-visible
370 wavelengths to the near-UV, calculated using Eq. 3. The AAE given by the power law exponent
371 reported in Figure 4a is 2.32 (1.35, 3.29; 95% confidence interval), indicating a significant
372 contribution of BrC to total absorption. The power law fits in Figure 4b yield $\text{AAE}_{\text{BrC}} = 6.26$

373 (5.37, 7.13) and $\text{AAE}_{\text{BC}} = 0.67$. For comparison, El Asmar et al. (2024) found similar overall
 374 $\text{AAE} = 1.89$ (range of 1.31–3.32) and a lower average $\text{AAE}_{\text{BrC}} = 5.00$ (range of 3.19–7.43) for
 375 prescribed burns in southeastern US measured 0–8 hours downwind with the same model
 376 multiwavelength aethalometer used in this study. The AAE_{BrC} for western wildfires measured
 377 with a photoacoustic spectrometer by Zeng et al. (2022) was also comparable (2.07 ± 1.01 ;
 378 average \pm standard deviation). Mie theory predicts that $\text{AAE}_{\text{BC}} = 1$ for particle diameters less
 379 than 10 nm and $\text{AAE}_{\text{BC}} < 1$ for particle diameters greater than $\sim 0.2 \mu\text{m}$ (Wang et al., 2016),
 380 suggesting that the bulk of sampled aerosols had a diameter greater than $0.2 \mu\text{m}$ and less than 2.5
 381 μm , since a $\text{PM}_{2.5}$ cyclone was placed on the sampling inlet.

382



383
 384 Figure 4: Average 1-minute absorption at seven wavelengths measured by the ground
 385 aethalometer plotted as red hexagons, with error bars representing 95% confidence intervals. (a)
 386 Power-law fit of the average absorption curve at all wavelengths with an $\text{AAE} = 2.32$ (solid
 387 curve) and a 95% confidence interval AAE values displayed as the bounding dashed curves by
 388 the shading between the dashed curves. (b) Power-law fit of the BrC average absorption curve (λ
 389 = 370, 470, 520, 590, and 660 nm; blue circles) with an $\text{AAE}_{\text{BrC}} = 6.26$ (solid brown curve)
 390 with and a 95% confidence interval AAE values displayed as the by the shading between
 391 the bounding dashed curves and the BC average absorptions ($\lambda = 880, 950$ nm; red hexagons)
 392 with an $\text{AAE}_{\text{BC}} = 0.67$ (solid black curve).
 393

394 Whereas the absorption cross-section of BrC is much lower than that of BC over the near-
 395 IR to near-UV portion of the solar spectrum, smoldering smoke emits much more BrC than BC:
 396 $7.0 \pm 2.7 \text{ gBrC kg}^{-1}$ versus $0.52 \pm 0.42 \text{ gBC kg}^{-1}$. Consequently, using Equation 5 and shown in
 397 Figure S10, we estimate that BrC and BC would account for 23% and 77% of incoming solar
 398 radiation absorbed by the smoldering smoke in the atmosphere (integrated from 300 to 2500
 399 nm). Furthermore, BrC would contribute 82% of the aerosol absorption of solar radiation at
 400 wavelengths below 400 nm and, therefore, may affect tropospheric photochemistry. [SimilarlyFor
401 ecomparison, Chakrabarty et al. \(2023\) found BrC contributes 66–86% of total aerosol absorption
402 at 405 nm in wildfire smoke emitted in the western United States.](#)

403 AAE values reported in the literature are computed using different approaches. For
 404 example, AAE is commonly derived from data at only two wavelengths and those wavelengths
 405 differ from study to study, which makes direct comparison among studies challenging. To
 406 illustrate this point, we calculated AAE values on 1-minute absorption data from the current
 407 study using three wavelength pairs that approximate prior work. Table 2 reports power law fitting
 408 of (i) 370 and 880 nm to approximate the wavelengths in a photoacoustic extintiometer, (ii) 470
 409 and 660 nm to approximate a continuous light absorption photometer, and (iii) 470 and 880 nm
 410 to approximate the satellite based AERONET.

411
 412 Table 2: Measured and Nearest Aethalometer Wavelengths to Calculate the Absorption Ångström
 413 Exponent (AAE)

Carbonaceous Aerosol Measurement Method	Example Studies	Measured Wavelengths, λ (nm)	Nearest Aethalometer Wavelengths, λ (nm)	AAE, Average \pm Standard Deviation
Aethalometer (Magee Scientific AE33)	This Work (Butler et al.) El Asmar et al. (2024)	370, 470, 520, 590, 660, 880, 950	—	2.55 ± 0.43
Photoacoustic spectrometer (Droplet Technologies PAX)	Selimovic et al. (2018) Zeng et al. (2022)	401, 870	370, 880	2.97 ± 0.54

Continuous light absorption photometer	Marsavin et al. (2023)	467, 652	470, 660	2.82 ± 0.59
Satellite (AERONET)	Cazorla et al. (2013) Feng et al. (2013) Wang et al. (2016) Bian et al. (2020)	440, 870	470, 880	2.15 ± 0.37

414

415 The 1-minute average AAE for the three wavelength pairs are listed in the rightmost
 416 column of Table 2. The 370, 880 and 470, 660~~880~~-wavelength pairs have a 16% and 11% greater
 417 value than the seven-wavelength power law fit in this work, whereas the 4740, ~~8870~~ wavelength
 418 pair a 16% lesser value. These differences in average AAE indicate the uncertainty in interstudy
 419 comparison is approximately $\pm 15\%$. Distributions of the coefficient of determination (r^2) for
 420 each approach are also presented in Figure S11. A power law fit of 1-minute average data at all
 421 seven wavelengths ($AAE_{7\lambda}$) yielded the highest average coefficient of determination ($r^2 = 0.88$),
 422 followed closely by fitting data at only 370 and 880 nm ($r^2 = 0.87$). The lower average r^2 values
 423 for power law fitting of data at 470 and 660 nm ($r^2 = 0.71$) and 470 and 880 nm ($r^2 = 0.60$)
 424 suggest that the AAE values determined from these approaches are not as certain.

425

426 4 Conclusion

427 Fuel-based BC and BrC emission factors were calculated by the carbon balance method
 428 with semi-continuous monitoring of a BC, CO, and CO₂ on ground and aerial platforms for four
 429 days of prescribed burns. Aerial platform BC emission factors were measured under both flaming
 430 and smoldering combustion, whereas ground platform BC and BrC emission factors skewed
 431 towards almost entirely under smoldering combustion conditions. AAE, an aerosol optical
 432 property, was similarly quantified for smoldering combustion. BC emission factors were found to
 433 be poorly represented by a linear regression model based on MCE and were 2 times higher under
 434 flaming combustion than smoldering combustion. In addition, BC emission factors may be used
 435 in smoke models to improve wildland fire emissions inventories. BrC emission factors, estimated
 436 using a BrC-specific absorption cross-section, were nearly 14 times greater than smoldering BC
 437 emission factors and 7 times greater than the smoldering and flaming BC emission factors,
 438 respectively. The study-average AAEs indicated significant BrC absorption, especially in the

439 near-UV spectrum, indicating that BrC is a significant contributor to biomass smoke absorption
440 of solar radiation. A fraction of this BrC absorption may be attributable to so-called BrC tar
441 balls, which may comprise 5–30% of total PM_{2.5} in wildfire smoke in the western United States
442 (Adachi et al., 2024; Chakrabarty et al., 2023). The AAE_{BrC} reported here may be parametrized
443 in global earth systems models to represent the contribution of BrC to total aerosol absorption of
444 incoming shortwave radiation for mixed-conifer prescribed burning. (Saleh, 2020).

445 In future work, deployment of a multiwavelength aethalometer on the aerial platform,
446 would allow for Delta-C and AAE analyses to estimate BrC emission factors and optical
447 properties under flaming combustion. Multiwavelength aerosol absorption measurements on an
448 aerial platform across a wide range of combustion conditions would yield more representative
449 BrC emission factors and AAE values, which would inform how to model BrC emissions during
450 different combustion phases in fuel consumption models. Studies that quantify health impacts of
451 prescribed burn smoke with a chemical transport model will benefit from fuel-based emission
452 factors in this work and could determine the exposure concentrations of BC and BrC in PM_{2.5}.
453 The overall radiative effects of BC and BrC remains uncertain due to large uncertainties in global
454 emissions inventories from wildland fires sources (Bond et al., 2013). Further improvements in
455 bottom-up carbonaceous aerosol emissions inventories would constrain satellite retrievals of
456 aerosol optical depth used to model aerosol scattering and absorption in global climate models.

457 To mitigate the health and climate impacts of BC and BrC emissions, prescribed burns
458 will be critical to promote climate-resilient, fire-adapted forest ecosystems. Prescribed burns
459 consume less fuel per burned area than wildfires by a factor of 2–4, emit less greenhouse gases
460 and climate pollutants, and have less severe smoke health impacts (Kelp et al., 2023; Kiely et al.,
461 2024; Ottmar, 2014). Further partnership between government agencies, private land owners,
462 and tribal nations will likely increase the frequency of and effectiveness of prescribed burns, and
463 thus possible health effects on downwind communities (Miller et al., 2020). As prescribed burns
464 increase in prevalence, Ce continued field measurements of emission factors with state-of-the-
465 science platforms should focus on characterizing generating emission factors and optical
466 properties for ecosystems commonly burned in the western United States, like the mixed-conifer
467 forests studied here, Ponderosa pine forests, coastal forests, chaparral shrublands, and oak
468 savannas. Carbonaceous aerosol emission factors for each of these ecosystems remain

469 understudied, especially for BrC, and likely vary across ecosystems depending on fuel moisture
470 content, fuel types, and combustion efficiency of burn. In parallel, future studies could also
471 investigate the toxicity of BC and BrC emitted by prescribed burns, which may vary depending
472 on combustion conditions and fuels burned. Emission factors and optical properties of a related
473 land management practice, iIndigenous fire stewardship, could be studied in particular, should be
474 centered in this aim, which uses controlled fire to change fire regimes in ecosystems to adapt to
475 climate change, encourage certain species growth, and increase resources to sustain indigenous
476 knowledge, cultural practices, and traditions (Lake and Christianson, 2019). and wildland fire
477 activity globally.

478

479 **Author Contribution**

480 **James D.A. Butler:** Conceptualization, Data Curation, Formal Analysis, Investigation,
481 Methodology, Resources, Visualization, Writing – original draft, Writing – review and editing.

482 **Afsara Tasnia:** Data Curation, Investigation, Methodology, Resources, Writing – review and
483 editing.

484 **Deep Sengupta:** Data Curation, Investigation, Methodology, Resources.

485 **Nathan Kreisberg:** Data Curation, Investigation, Methodology, Resources, Writing – review
486 and editing.

487 **Kelley C. Barsanti:** Conceptualization, Funding Acquisition, Methodology, Project
488 Administration, Supervision, Writing – review and editing.

489 **Allen H Goldstein:** Conceptualization, Funding Acquisition, Methodology, Project
490 Administration, Supervision, Writing – review and editing.

491 **Chelsea V. Preble:** Conceptualization, Methodology, Resources, Writing – review and editing.

492 **Rebecca A. Sugrue:** Resources, Writing – review and editing.

493 **Thomas W. Kirchstetter:** Conceptualization, Funding Acquisition, Methodology, Writing –
494 original draft, Writing – review and editing.

495

496 **Competing interests**

497 We declare that co-author Barsanti is on the editorial board of the journal *Atmospheric Chemistry*
498 and *Physics*.

499

500 **Code/Data Availability**

501 Data and code available upon request.

502

503 **Acknowledgement**

504 This work was supported by the California Air Resources Board (CARB) under contract
505 19RD008 and the California Department of Forestry and Fire Protection (CAL FIRE). Butler,
506 Kirchstetter, Preble, and Sugrue also acknowledge support of the Department of Energy under
507 Contract No. DEAC02-05CH11231. The statements and conclusions herein are those of the
508 authors and do not necessarily reflect the views of the project sponsors. We thank Ariel
509 Roughton, Rob York, John Battles, Scott Stephens and the staff of the Blodgett Forest Research
510 Station for their work to conduct the prescribed burns, feed and house the research team, and
511 ensure safety when taking field measurements; Coty Jen for her feedback on early analyses;
512 Drew Hill for his assistance on the Delta-C methodology; Adam Wise for development of the
513 photographs in Key Figure, Figure S2, and Figure S9; and Robert Harley for his review of early
514 drafts.

515

516 **References**

517 [Adachi, K., Dibb, J. E., Katich, J. M., Schwarz, J. P., Guo, H., Campuzano-Jost, P., Jimenez, J. L., Peischl, J., Holmes, C. D., and Crawford, J.: Occurrence, abundance, and formation of atmospheric tarballs from a wide range of wildfires in the western US, Atmospheric Chemistry and Physics, 24, 10985–11004, <https://doi.org/10.5194/acp-24-10985-2024>, 2024.](https://doi.org/10.5194/acp-24-10985-2024)

521 [Aerosol d.o.o.: Aethalometer\(R\) - AE36s: Expand the fronteirs of aerosol Science with cutting-edge Black Carbon instrument, Aerosol Magee Scientific, Ljubljana, Slovenia, 2024.](https://doi.org/10.5194/acp-24-10985-2024)

523 [Akagi, S. K., Yokelson, R. J., Wiedinmyer, C., Alvarado, M. J., Reid, J. S., Karl, T., Crounse, J. D., and Wennberg, P. O.: Emission factors for open and domestic biomass burning for use in atmospheric models, Atmospheric Chemistry and Physics, 11, 4039–4072, <https://doi.org/10.5194/acp-11-4039-2011>, 2011.](https://doi.org/10.5194/acp-11-4039-2011)

527 [Andreae, M. O.: Emission of trace gases and aerosols from biomass burning – an updated assessment, Atmospheric Chemistry and Physics, 19, 8523–8546, <https://doi.org/10.5194/acp-19-8523-2019>, 2019.](https://doi.org/10.5194/acp-19-8523-2019)

530 [Aurell, J. and Gullett, B. K.: Emission Factors from Aerial and Ground Measurements of Field and Laboratory Forest Burns in the Southeastern U.S.: PM2.5, Black and Brown Carbon, VOC,](https://doi.org/10.5194/acp-24-10985-2024)

- 532 and PCDD/PCDF, *Environ. Sci. Technol.*, 47, 8443–8452, <https://doi.org/10.1021/es402101k>,
533 2013.
- 534 [Aurell, J., Gullett, B., Holder, A., Kiros, F., Mitchell, W., Watts, A., and Ottmar, R.: Wildland fire](#)
535 [emission sampling at Fishlake National Forest, Utah using an unmanned aircraft system,](#)
536 [Atmospheric Environment, 247, 118193, https://doi.org/10.1016/j.atmosenv.2021.118193, 2021.](#)
- 537 [Bian, Q., Ford, B., Pierce, J. R., and Kreidenweis, S. M.: A Decadal Climatology of Chemical,](#)
538 [Physical, and Optical Properties of Ambient Smoke in the Western and Southeastern United](#)
539 [States, *Journal of Geophysical Research: Atmospheres*, 125, e2019JD031372,](#)
540 [https://doi.org/10.1029/2019JD031372, 2020.](#)
- 541 [Binte Shahid, S., Lacey, F. G., Wiedinmyer, C., Yokelson, R. J., and Barsanti, K. C.: NEIVAv1.0:](#)
542 [Next-generation Emissions InVentory expansion of Akagi et al. \(2011\) version 1.0, *Geoscientific*](#)
543 [Model Development, 17, 7679–7711, https://doi.org/10.5194/gmd-17-7679-2024, 2024.](#)
- 544 [Bond, T. C., Streets, D. G., Yarber, K. F., Nelson, S. M., Woo, J.-H., and Klimont, Z.: A](#)
545 [technology-based global inventory of black and organic carbon emissions from combustion,](#)
546 [Journal of Geophysical Research: Atmospheres, 109, https://doi.org/10.1029/2003JD003697,](#)
547 [2004.](#)
- 548 [Bond, T. C., Doherty, S. J., Fahey, D. W., Forster, P. M., Berntsen, T., DeAngelo, B. J., Flanner,](#)
549 [M. G., Ghan, S., Kärcher, B., Koch, D., Kinne, S., Kondo, Y., Quinn, P. K., Sarofim, M. C.,](#)
550 [Schultz, M. G., Schulz, M., Venkataraman, C., Zhang, H., Zhang, S., Bellouin, N., Guttikunda, S.](#)
551 [K., Hopke, P. K., Jacobson, M. Z., Kaiser, J. W., Klimont, Z., Lohmann, U., Schwarz, J. P.,](#)
552 [Shindell, D., Storelvmo, T., Warren, S. G., and Zender, C. S.: Bounding the role of black carbon](#)
553 [in the climate system: A scientific assessment, *Journal of Geophysical Research: Atmospheres*,](#)
554 [118, 5380–5552, https://doi.org/10.1002/jgrd.50171, 2013.](#)
- 555 [Burling, I. R., Yokelson, R. J., Akagi, S. K., Urbanski, S. P., Wold, C. E., Griffith, D. W. T.,](#)
556 [Johnson, T. J., Reardon, J., and Weise, D. R.: Airborne and ground-based measurements of the](#)
557 [trace gases and particles emitted by prescribed fires in the United States, *Atmospheric Chemistry*](#)
558 [and Physics, 11, 12197–12216, https://doi.org/10.5194/acp-11-12197-2011, 2011.](#)
- 559 [California Air Resources Board: California's Black Carbon Emission Inventory–Technical](#)
560 [Support Document, 2016.](#)
- 561 [California Air Resources Board: Greenhouse Gas Emissions of Contemporary Wildfire,](#)
562 [Prescribed Fire, and Forest Management Activities, California Air Resources Board, Sacramento,](#)
563 [CA, 2020.](#)
- 564 [Caubel, J. J., Cados, T. E., and Kirchstetter, T. W.: A new black carbon sensor for dense air](#)
565 [quality monitoring networks, *Sensors*, 18, 738, https://doi.org/10.3390/s18030738, 2018.](#)
- 566 [Cazorla, A., Bahadur, R., Suski, K. J., Cahill, J. F., Chand, D., Schmid, B., Ramanathan, V., and](#)
567 [Prather, K. A.: Relating aerosol absorption due to soot, organic carbon, and dust to emission](#)

- 568 [sources determined from in-situ chemical measurements, Atmospheric Chemistry and Physics, 13, 9337–9350, <https://doi.org/10.5194/acp-13-9337-2013>, 2013.](https://doi.org/10.5194/acp-13-9337-2013)
- 570 [Chakrabarty, R. K., Shetty, N. J., Thind, A. S., Beeler, P., Sumlin, B. J., Zhang, C., Liu, P., Idrobo, J. C., Adachi, K., Wagner, N. L., Schwarz, J. P., Ahern, A., Sedlacek, A. J., Lambe, A., Daube, C., Lyu, M., Liu, C., Herndon, S., Onasch, T. B., and Mishra, R.: Shortwave absorption by wildfire smoke dominated by dark brown carbon, Nat. Geosci., 16, 683–688, <https://doi.org/10.1038/s41561-023-01237-9>, 2023.](https://doi.org/10.1038/s41561-023-01237-9)
- 575 [Chelluboyina, G. S., Kapoor, T. S., and Chakrabarty, R. K.: Dark brown carbon from wildfires: a potent snow radiative forcing agent?, npj Clim Atmos Sci, 7, 1–10, <https://doi.org/10.1038/s41612-024-00738-7>, 2024.](https://doi.org/10.1038/s41612-024-00738-7)
- 576
- 577
- 578 [Chen, L.-W. A., Moosmüller, H., Arnott, W. P., Chow, J. C., Watson, J. G., Susott, R. A., Babbitt, R. E., Wold, C. E., Lincoln, E. N., and Hao, W. M.: Emissions from Laboratory Combustion of Wildland Fuels: Emission Factors and Source Profiles, Environ. Sci. Technol., 41, 4317–4325, <https://doi.org/10.1021/es062364i>, 2007.](https://doi.org/10.1021/es062364i)
- 579
- 580
- 581
- 582 [Chow, J. C., Watson, J. G., Lowenthal, D. H., Antony Chen, L.-W., and Motallebi, N.: PM2.5 source profiles for black and organic carbon emission inventories, Atmospheric Environment, 45, 5407–5414, <https://doi.org/10.1016/j.atmosenv.2011.07.011>, 2011.](https://doi.org/10.1016/j.atmosenv.2011.07.011)
- 583
- 584
- 585 [Connolly, R., Marlier, M. E., Garcia-Gonzales, D. A., Wilkins, J., Su, J., Bekker, C., Jung, J., Bonilla, E., Burnett, R. T., Zhu, Y., and Jerrett, M.: Mortality attributable to PM2.5 from wildland fires in California from 2008 to 2018, Science Advances, 10, eadl1252, <https://doi.org/10.1126/sciadv.adl1252>, 2024.](https://doi.org/10.1126/sciadv.adl1252)
- 586
- 587
- 588
- 589 [Cruz Núñez, X., Villers Ruiz, L., and Gay García, C.: Black carbon and organic carbon emissions from wildfires in Mexico, Atmósfera, 27, 165–172, \[https://doi.org/10.1016/S0187-6236\\(14\\)71107-5\]\(https://doi.org/10.1016/S0187-6236\(14\)71107-5\), 2014.](https://doi.org/10.1016/S0187-6236(14)71107-5)
- 590
- 591
- 592 [Dong, Q., Meng, X., Gong, J., and Zhu, T.: A review of advances in black carbon exposure assessment and health effects, CSB, 69, 703–716, <https://doi.org/10.1360/TB-2023-0409>, 2023.](https://doi.org/10.1360/TB-2023-0409)
- 593
- 594 [El Asmar, R., Li, Z., Tanner, D. J., Hu, Y., O'Neill, S., Huey, L. G., Odman, M. T., and Weber, R. J.: A multi-site passive approach to studying the emissions and evolution of smoke from prescribed fires, Atmospheric Chemistry and Physics, 24, 12749–12773, <https://doi.org/10.5194/acp-24-12749-2024>, 2024.](https://doi.org/10.5194/acp-24-12749-2024)
- 595
- 596
- 597
- 598 [Feng, Y., Ramanathan, V., and Kotamarthi, V. R.: Brown carbon: a significant atmospheric absorber of solar radiation?, Atmospheric Chemistry and Physics, 13, 8607–8621, <https://doi.org/10.5194/acp-13-8607-2013>, 2013.](https://doi.org/10.5194/acp-13-8607-2013)
- 599
- 600
- 601 [Grahame, T. J., Klemm, R., and Schlesinger, R. B.: Public health and components of particulate matter: The changing assessment of black carbon, Journal of the Air & Waste Management Association, 64, 620–660, <https://doi.org/10.1080/10962247.2014.912692>, 2014.](https://doi.org/10.1080/10962247.2014.912692)
- 602
- 603

- 604 [Hadley, O. L. and Kirchstetter, T. W.: Black-carbon reduction of snow albedo, Nature Clim
605 Change, 2, 437–440, <https://doi.org/10.1038/nclimate1433>, 2012.](https://doi.org/10.1038/nclimate1433)
- 606 [Harrison, R. M., Beddows, D. C. S., Jones, A. M., Calvo, A., Alves, C., and Pio, C.: An
607 evaluation of some issues regarding the use of aethalometers to measure woodsmoke
608 concentrations, Atmospheric Environment, 80, 540–548,
609 <https://doi.org/10.1016/j.atmosenv.2013.08.026>, 2013.](https://doi.org/10.1016/j.atmosenv.2013.08.026)
- 610 [Hosseini, S., Urbanski, S. P., Dixit, P., Qi, L., Burling, I. R., Yokelson, R. J., Johnson, T. J.,
611 Shrivastava, M., Jung, H. S., Weise, D. R., Miller, J. W., and Cocker III, D. R.: Laboratory
612 characterization of PM emissions from combustion of wildland biomass fuels, Journal of
613 Geophysical Research: Atmospheres, 118, 9914–9929, <https://doi.org/10.1002/jgrd.50481>, 2013.](https://doi.org/10.1002/jgrd.50481)
- 614 [Huang, J., Hopke, P. K., Choi, H.-D., Laing, J. R., Cui, H., Zananski, T. J., Chandrasekaran, S.
615 Rattigan, O. V., and Holsen, T. M.: Mercury \(Hg\) emissions from domestic biomass
616 combustion for space heating, Chemosphere, 84, 1694–1699,
617 <https://doi.org/10.1016/j.chemosphere.2011.04.078>, 2011.](https://doi.org/10.1016/j.chemosphere.2011.04.078)
- 618 [Ivančič, M., Gregorič, A., Lavrič, G., Alföldy, B., Ježek, I., Hasheminassab, S., Pakbin, P.,
619 Ahangar, F., Sowlat, M., Boddeker, S., and Rigler, M.: Two-year-long high-time-resolution
620 apportionment of primary and secondary carbonaceous aerosols in the Los Angeles Basin using
621 an advanced total carbon–black carbon \(TC-BC\(\$\lambda\$ \)\) method, Science of The Total Environment,
622 848, 157606, <https://doi.org/10.1016/j.scitotenv.2022.157606>, 2022.](https://doi.org/10.1016/j.scitotenv.2022.157606)
- 623 [Janssen, N. A. H., Hoek, G., Simic-Lawson, M., Fischer, P., van Bree, L., ten Brink, H., Keuken,
624 M., Atkinson, R. W., Anderson, H. R., Brunekreef, B., and Cassee, F. R.: Black carbon as an
625 additional indicator of the adverse health effects of airborne particles compared with PM10 and
626 PM2.5, Environ Health Perspect, 119, 1691–1699, <https://doi.org/10.1289/ehp.1003369>, 2011.](https://doi.org/10.1289/ehp.1003369)
- 627 [Kaspari, S., McKenzie Skiles, S., Delaney, I., Dixon, D., and Painter, T. H.: Accelerated glacier
628 melt on Snow Dome, Mount Olympus, Washington, USA, due to deposition of black carbon and
629 mineral dust from wildfire, Journal of Geophysical Research: Atmospheres, 120, 2793–2807,
630 <https://doi.org/10.1002/2014JD022676>, 2015.](https://doi.org/10.1002/2014JD022676)
- 631 [Keane, R. E. and Lutes, D.: First-Order Fire Effects Model \(FOFEM\), in: Encyclopedia of
632 Wildfires and Wildland-Urban Interface \(WUI\) Fires, edited by: Manzello, S. L., Springer
633 International Publishing, Cham, 1–5, \[https://doi.org/10.1007/978-3-319-51727-8_74-1\]\(https://doi.org/10.1007/978-3-319-51727-8_74-1\), 2018.](https://doi.org/10.1007/978-3-319-51727-8_74-1)
- 634 [Kirchstetter, T. W. and Thatcher, T. L.: Contribution of organic carbon to wood smoke particulate
635 matter absorption of solar radiation, Atmospheric Chemistry and Physics, 12, 6067–6072,
636 <https://doi.org/10.5194/acp-12-6067-2012>, 2012.](https://doi.org/10.5194/acp-12-6067-2012)
- 637 [Kirchstetter, T. W., Novakov, T., and Hobbs, P. V.: Evidence that the spectral dependence of light
638 absorption by aerosols is affected by organic carbon, Journal of Geophysical Research:
639 Atmospheres, 109, <https://doi.org/10.1029/2004JD004999>, 2004.](https://doi.org/10.1029/2004JD004999)

- 640 [Larkin, N. K., Raffuse, S. M., Huang, S., Pavlovic, N., Lahm, P., and Rao, V.: The](#)
641 [Comprehensive Fire Information Reconciled Emissions \(CFIRE\) inventory: Wildland fire](#)
642 [emissions developed for the 2011 and 2014 U.S. National Emissions Inventory, Journal of the](#)
643 [Air & Waste Management Association, 70, 1165–1185,](#)
644 [https://doi.org/10.1080/10962247.2020.1802365, 2020.](https://doi.org/10.1080/10962247.2020.1802365)
- 645 [BlueSky Modeling Framework: https://www.airfire.org/data/bluesky, last access: 12 November](#)
646 [2024.](#)
- 647 [Laskin, A., Laskin, J., and Nizkorodov, S. A.: Chemistry of Atmospheric Brown Carbon, Chem.](#)
648 [Rev., 115, 4335–4382, https://doi.org/10.1021/cr5006167, 2015.](https://doi.org/10.1021/cr5006167)
- 649 [Levinson, R., Akbari, H., and Berdahl, P.: Measuring solar reflectance—Part I: Defining a metric](#)
650 [that accurately predicts solar heat gain, Solar Energy, 84, 1717–1744,](#)
651 [https://doi.org/10.1016/j.solener.2010.04.018, 2010.](https://doi.org/10.1016/j.solener.2010.04.018)
- 652 [Li, J. and Li, Y.: Ozone deterioration over North China plain caused by light absorption of black](#)
653 [carbon and organic carbon, Atmospheric Environment, 313, 120048,](#)
654 [https://doi.org/10.1016/j.atmosenv.2023.120048, 2023.](https://doi.org/10.1016/j.atmosenv.2023.120048)
- 655 [Liu, C., Chung, C. E., Yin, Y., and Schnaiter, M.: The absorption Ångström exponent of black](#)
656 [carbon: from numerical aspects, Atmospheric Chemistry and Physics, 18, 6259–6273,](#)
657 [https://doi.org/10.5194/acp-18-6259-2018, 2018.](https://doi.org/10.5194/acp-18-6259-2018)
- 658 [Lutes, D. C.: FOFEM 6.7 User Guide, United States Forest Service, 2020.](#)
- 659 [Maji, K. J., Li, Z., Vaidyanathan, A., Hu, Y., Stowell, J. D., Milano, C., Wellenius, G., Kinney,](#)
660 [P. L., Russell, A. G., and Odman, M. T.: Estimated Impacts of Prescribed Fires on Air Quality](#)
661 [and Premature Deaths in Georgia and Surrounding Areas in the US, 2015–2020, Environ. Sci.](#)
662 [Technol., https://doi.org/10.1021/acs.est.4c00890, 2024.](https://doi.org/10.1021/acs.est.4c00890)
- 663 [Marsavin, A., Gageldonk, R. van, Bernays, N., May, N. W., Jaffe, D. A., and Fry, J. L.: Optical](#)
664 [properties of biomass burning aerosol during the 2021 Oregon fire season: comparison between](#)
665 [wild and prescribed fires, Environ. Sci.: Atmos., 3, 608–626,](#)
666 [https://doi.org/10.1039/D2EA00118G, 2023.](https://doi.org/10.1039/D2EA00118G)
- 667 [May, A. A., McMeeking, G. R., Lee, T., Taylor, J. W., Craven, J. S., Burling, I., Sullivan, A. P.,](#)
668 [Akagi, S., Collett, J. L., Flynn, M., Coe, H., Urbanski, S. P., Seinfeld, J. H., Yokelson, R. J., and](#)
669 [Kreidenweis, S. M.: Aerosol emissions from prescribed fires in the United States: A synthesis of](#)
670 [laboratory and aircraft measurements, Journal of Geophysical Research: Atmospheres, 119,](#)
671 [11,826–11,849, https://doi.org/10.1002/2014JD021848, 2014.](https://doi.org/10.1002/2014JD021848)
- 672 [McMeeking, G. R., Kreidenweis, S. M., Baker, S., Carrico, C. M., Chow, J. C., Collett, J. L.,](#)
673 [Hao, W. M., Holden, A. S., Kirchstetter, T. W., Malm, W. C., Moosmüller, H., Sullivan, A. P., and](#)
674 [Wold, C. E.: Emissions of trace gases and aerosols during the open combustion of biomass in the](#)

- 675 [laboratory, Journal of Geophysical Research: Atmospheres, 114,](https://doi.org/10.1029/2009JD011836)
676 [https://doi.org/10.1029/2009JD011836, 2009.](https://doi.org/10.1029/2009JD011836)
- 677 [Miller, R. K., Field, C. B., and Mach, K. J.: Barriers and enablers for prescribed burns for](https://doi.org/10.1038/s41893-019-0451-7)
678 [wildfire management in California, Nat Sustain, 3, 101–109, https://doi.org/10.1038/s41893-019-](https://doi.org/10.1038/s41893-019-0451-7)
679 [0451-7, 2020.](https://doi.org/10.1038/s41893-019-0451-7)
- 680 [Mok, J., Krotkov, N. A., Arola, A., Torres, O., Jethva, H., Andrade, M., Labow, G., Eck, T. F., Li,](https://doi.org/10.1038/srep36940)
681 [Z., Dickerson, R. R., Stenchikov, G. L., Osipov, S., and Ren, X.: Impacts of brown carbon from](https://doi.org/10.1038/srep36940)
682 [biomass burning on surface UV and ozone photochemistry in the Amazon Basin, Sci Rep, 6,](https://doi.org/10.1038/srep36940)
683 [36940, https://doi.org/10.1038/srep36940, 2016.](https://doi.org/10.1038/srep36940)
- 684 [Nelson Jr., R. M.: An evaluation of the carbon balance technique for estimating emission factors](https://doi.org/10.2737/SE-RP-231)
685 [and fuel consumption in forest fires, Res. Pap. SE-231. Asheville, NC: U.S. Department of](https://doi.org/10.2737/SE-RP-231)
686 [Agriculture, Forest Service, Southeastern Forest Experiment Station, 231, 9,](https://doi.org/10.2737/SE-RP-231)
687 [https://doi.org/10.2737/SE-RP-231, 1982.](https://doi.org/10.2737/SE-RP-231)
- 688 [North, M., Collins, B., Safford, H., and Stephenson, N.: Montane Forests, in: Ecosystems of](https://doi.org/10.1080/15414319.2016.117292)
689 [California, University of California Press, 553–578, 2016.](https://doi.org/10.1080/15414319.2016.117292)
- 690 [Ottmar, R. D.: Wildland fire emissions, carbon, and climate: Modeling fuel consumption, Forest](https://doi.org/10.1016/j.foreco.2013.06.010)
691 [Ecology and Management, 317, 41–50, https://doi.org/10.1016/j.foreco.2013.06.010, 2014.](https://doi.org/10.1016/j.foreco.2013.06.010)
- 692 [Selimovic, V., Yokelson, R. J., Warneke, C., Roberts, J. M., de Gouw, J., Reardon, J., and](https://doi.org/10.5194/acp-18-2929-2018)
693 [Griffith, D. W. T.: Aerosol optical properties and trace gas emissions by PAX and OP-FTIR for](https://doi.org/10.5194/acp-18-2929-2018)
694 [laboratory-simulated western US wildfires during FIREX, Atmospheric Chemistry and Physics,](https://doi.org/10.5194/acp-18-2929-2018)
695 [18, 2929–2948, https://doi.org/10.5194/acp-18-2929-2018, 2018.](https://doi.org/10.5194/acp-18-2929-2018)
- 696 [Stampfer, O., Austin, E., Ganuelas, T., Fiander, T., Seto, E., and Karr, C. J.: Use of low-cost PM](https://doi.org/10.1016/j.atmosenv.2020.117292)
697 [monitors and a multi-wavelength aethalometer to characterize PM2.5 in the Yakama Nation](https://doi.org/10.1016/j.atmosenv.2020.117292)
698 [reservation, Atmospheric Environment, 224, 117292,](https://doi.org/10.1016/j.atmosenv.2020.117292)
699 [https://doi.org/10.1016/j.atmosenv.2020.117292, 2020.](https://doi.org/10.1016/j.atmosenv.2020.117292)
- 700 [Steel, Z. L., Foster, D., Coppoletta, M., Lydersen, J. M., Stephens, S. L., Paudel, A., Markwith,](https://doi.org/10.1111/1365-2745.13764)
701 [S. H., Merriam, K., and Collins, B. M.: Ecological resilience and vegetation transition in the face](https://doi.org/10.1111/1365-2745.13764)
702 [of two successive large wildfires, Journal of Ecology, 109, 3340–3355,](https://doi.org/10.1111/1365-2745.13764)
703 [https://doi.org/10.1111/1365-2745.13764, 2021.](https://doi.org/10.1111/1365-2745.13764)
- 704 [Sugrue, R. A., Preble, C. V., Butler, J. D. A., Redon-Gabel, A. J., Marconi, P., Shetty, K. D., Hill,](https://doi.org/10.1016/j.atmosenv.2024.120434)
705 [L. A. L., Amezcua-Smith, A. M., Lukyanov, B. R., and Kirchstetter, T. W.: The value of adding](https://doi.org/10.1016/j.atmosenv.2024.120434)
706 [black carbon to community monitoring of particulate matter, Atmospheric Environment, 325,](https://doi.org/10.1016/j.atmosenv.2024.120434)
707 [120434, https://doi.org/10.1016/j.atmosenv.2024.120434, 2024.](https://doi.org/10.1016/j.atmosenv.2024.120434)
- 708 [Tasnja, A., Lara, G., Foster, D., Sengupta, D., Butler, J. D. A., Kirchstetter, T. W., York, R.,](https://doi.org/10.1016/j.atmosenv.2024.120434)
709 [Kreisberg, N. M., Goldstein, A. H., Battles, J. J., and Barsanti, K. C.: Comprehensive Fuel and](https://doi.org/10.1016/j.atmosenv.2024.120434)

- 710 [Emissions Measurements Highlight Uncertainties in Smoke Production Using Predictive
711 Modeling Tools, ACS EST Air, 2, 982–997, <https://doi.org/10.1021/acsestair.4c00142>, 2025.](https://doi.org/10.1021/acsestair.4c00142)
- 712 [Thomas, S. C. and Martin, A. R.: Carbon Content of Tree Tissues: A Synthesis, Forests, 3, 332–
713 352, <https://doi.org/10.3390/f3020332>, 2012.](https://doi.org/10.3390/f3020332)
- 714 [Urbanski, S.: Wildland fire emissions, carbon, and climate: Emission factors, Forest Ecology and
715 Management, 317, 51–60, <https://doi.org/10.1016/j.foreco.2013.05.045>, 2014.](https://doi.org/10.1016/j.foreco.2013.05.045)
- 716 [Urbanski, S. P., Hao, W. M., and Baker, S.: Chapter 4 Chemical Composition of Wildland Fire
717 Emissions, in: Developments in Environmental Science, vol. 8, edited by: Bytnerowicz, A.,
718 Arbaugh, M. J., Riebau, A. R., and Andersen, C., Elsevier, 79–107,
719 \[https://doi.org/10.1016/S1474-8177\\(08\\)00004-1\]\(https://doi.org/10.1016/S1474-8177\(08\)00004-1\), 2008.](https://doi.org/10.1016/S1474-8177(08)00004-1)
- 720 [US Environmental Protection Agency: 2020 National Emissions Inventory Technical Support
721 Document: Fires –Wild, Prescribed, and Agricultural Field Burning, US Environmental
722 Protection Agency, Research Triangle Park, NC, 2023.](https://www.epa.gov/air-emissions-modeling/speciate-0)
- 723 [SPECIATE: <https://www.epa.gov/air-emissions-modeling/speciate-0>, last access: 16 January
724 2025.](https://www.epa.gov/air-emissions-modeling/speciate-0)
- 725 [Wagstaff, M., Henderson, S. B., McLean, K. E., and Brauer, M.: Development of methods for
726 citizen scientist mapping of residential woodsmoke in small communities, Journal of
727 Environmental Management, 311, 114788, <https://doi.org/10.1016/j.jenvman.2022.114788>, 2022.](https://doi.org/10.1016/j.jenvman.2022.114788)
- 728 [Wang, X., Heald, C. L., Sedlacek, A. J., de Sá, S. S., Martin, S. T., Alexander, M. L., Watson, T.
729 B., Aiken, A. C., Springston, S. R., and Artaxo, P.: Deriving brown carbon from multiwavelength
730 absorption measurements: method and application to AERONET and Aethalometer observations,
731 Atmospheric Chemistry and Physics, 16, 12733–12752, <https://doi.org/10.5194/acp-16-12733-2016>, 2016.](https://doi.org/10.5194/acp-16-12733-2016)
- 733 [Wang, Y., Huang, J., Zananski, T. J., Hopke, P. K., and Holsen, T. M.: Impacts of the Canadian
734 Forest Fires on Atmospheric Mercury and Carbonaceous Particles in Northern New York,
735 Environ. Sci. Technol., 44, 8435–8440, <https://doi.org/10.1021/es1024806>, 2010.](https://doi.org/10.1021/es1024806)
- 736 [Wang, Y., Hopke, P. K., Rattigan, O. V., Xia, X., Chalupa, D. C., and Utell, M. J.:
737 Characterization of Residential Wood Combustion Particles Using the Two-Wavelength
738 Aethalometer, Environ. Sci. Technol., 45, 7387–7393, <https://doi.org/10.1021/es2013984>, 2011a.](https://doi.org/10.1021/es2013984)
- 739 [Wang, Y., Hopke, P. K., and Utell, M. J.: Urban-scale Spatial-temporal Variability of Black
740 Carbon and Winter Residential Wood Combustion Particles, Aerosol Air Qual. Res., 11, 473–
741 481, <https://doi.org/10.4209/aaqr.2011.01.0005>, 2011b.](https://doi.org/10.4209/aaqr.2011.01.0005)
- 742 [Ward, D. E. and Radke, L. F.: Emissions Measurements from Vegetation Fires: A Comparative
743 Evaluation of Methods and Results, in: Fire in the Environment: The Ecological, Atmospheric,
744 and Climatic Importance of Vegetation Fires, John Wiley & Sons Ltd., 53–76, 1993.](https://doi.org/10.1002/9780470971279.ch1)

- 745 [Wiedinmyer, C., Quayle, B., Geron, C., Belote, A., McKenzie, D., Zhang, X., O'Neill, S., and](https://doi.org/10.1016/j.atmosenv.2006.02.010)
746 [Wynne, K. K.: Estimating emissions from fires in North America for air quality modeling,](https://doi.org/10.1016/j.atmosenv.2006.02.010)
747 [Atmospheric Environment, 40, 3419–3432, https://doi.org/10.1016/j.atmosenv.2006.02.010,](https://doi.org/10.1016/j.atmosenv.2006.02.010)
748 [2006.](https://doi.org/10.1016/j.atmosenv.2006.02.010)
- 749 [Wu, X., Sverdrup, E., Mastrandrea, M. D., Wara, M. W., and Wager, S.: Low-intensity fires](https://doi.org/10.1126/sciadv.adi4123)
750 [mitigate the risk of high-intensity wildfires in California's forests, Science Advances, 9,](https://doi.org/10.1126/sciadv.adi4123)
751 [eadi4123, https://doi.org/10.1126/sciadv.adi4123, 2023.](https://doi.org/10.1126/sciadv.adi4123)
- 752 [Yang, S., Xu, B., Cao, J., Zender, C. S., and Wang, M.: Climate effect of black carbon aerosol in](https://doi.org/10.1016/j.atmosenv.2015.03.016)
753 [a Tibetan Plateau glacier, Atmospheric Environment, 111, 71–78,](https://doi.org/10.1016/j.atmosenv.2015.03.016)
754 [https://doi.org/10.1016/j.atmosenv.2015.03.016, 2015.](https://doi.org/10.1016/j.atmosenv.2015.03.016)
- 755 [Yokelson, R. J., Burling, I. R., Gilman, J. B., Warneke, C., Stockwell, C. E., de Gouw, J., Akagi,](https://doi.org/10.5194/acp-13-89-2013)
756 [S. K., Urbanski, S. P., Veres, P., Roberts, J. M., Kuster, W. C., Reardon, J., Griffith, D. W. T.,](https://doi.org/10.5194/acp-13-89-2013)
757 [Johnson, T. J., Hosseini, S., Miller, J. W., Cocker III, D. R., Jung, H., and Weise, D. R.: Coupling](https://doi.org/10.5194/acp-13-89-2013)
758 [field and laboratory measurements to estimate the emission factors of identified and unidentified](https://doi.org/10.5194/acp-13-89-2013)
759 [trace gases for prescribed fires, Atmospheric Chemistry and Physics, 13, 89–116,](https://doi.org/10.5194/acp-13-89-2013)
760 [https://doi.org/10.5194/acp-13-89-2013, 2013.](https://doi.org/10.5194/acp-13-89-2013)
- 761 [Zeng, L., Dibb, J., Scheuer, E., Katich, J. M., Schwarz, J. P., Bourgeois, I., Peischl, J., Ryerson,](https://doi.org/10.5194/acp-22-8009-2022)
762 [T., Warneke, C., Perring, A. E., Diskin, G. S., DiGangi, J. P., Nowak, J. B., Moore, R. H.,](https://doi.org/10.5194/acp-22-8009-2022)
763 [Wiggins, E. B., Pagonis, D., Guo, H., Campuzano-Jost, P., Jimenez, J. L., Xu, L., and Weber, R.](https://doi.org/10.5194/acp-22-8009-2022)
764 [J.: Characteristics and evolution of brown carbon in western United States wildfires,](https://doi.org/10.5194/acp-22-8009-2022)
765 [Atmospheric Chemistry and Physics, 22, 8009–8036, https://doi.org/10.5194/acp-22-8009-2022,](https://doi.org/10.5194/acp-22-8009-2022)
766 [2022.](https://doi.org/10.5194/acp-22-8009-2022)
- 767 [Zhang, A., Wang, Y., Zhang, Y., Weber, R. J., Song, Y., Ke, Z., and Zou, Y.: Modeling the global](https://doi.org/10.5194/acp-20-1901-2020)
768 [radiative effect of brown carbon: a potentially larger heating source in the tropical free](https://doi.org/10.5194/acp-20-1901-2020)
769 [troposphere than black carbon, Atmospheric Chemistry and Physics, 20, 1901–1920,](https://doi.org/10.5194/acp-20-1901-2020)
770 [https://doi.org/10.5194/acp-20-1901-2020, 2020.](https://doi.org/10.5194/acp-20-1901-2020)
- 771 [Adachi, K., Dibb, J. E., Katich, J. M., Schwarz, J. P., Guo, H., Campuzano-Jost, P., Jimenez, J.](https://doi.org/10.5194/acp-24-10985-2024)
772 [L., Peischl, J., Holmes, C. D., and Crawford, J.: Occurrence, abundance, and formation of](https://doi.org/10.5194/acp-24-10985-2024)
773 [atmospheric tarballs from a wide range of wildfires in the western US, Atmospheric Chemistry](https://doi.org/10.5194/acp-24-10985-2024)
774 [and Physics, 24, 10985–11004, https://doi.org/10.5194/acp-24-10985-2024, 2024.](https://doi.org/10.5194/acp-24-10985-2024)
- 775 [Aerosol d.o.o.: Aethalometer\(R\) AE36s: Expand the frontiers of aerosol Science with cutting-](https://doi.org/10.5194/acp-11-4039-2011)
776 [edge Black Carbon instrument, Aerosol Magee Scientific, Ljubljana, Slovenia, 2024.](https://doi.org/10.5194/acp-11-4039-2011)
- 777 [Akagi, S. K., Yokelson, R. J., Wiedinmyer, C., Alvarado, M. J., Reid, J. S., Karl, T., Crounse, J.](https://doi.org/10.5194/acp-11-4039-2011)
778 [D., and Wennberg, P. O.: Emission factors for open and domestic biomass burning for use in](https://doi.org/10.5194/acp-11-4039-2011)
779 [atmospheric models, Atmospheric Chemistry and Physics, 11, 4039–4072,](https://doi.org/10.5194/acp-11-4039-2011)
780 [https://doi.org/10.5194/acp-11-4039-2011, 2011.](https://doi.org/10.5194/acp-11-4039-2011)

- 781 [Andreae, M. O.: Emission of trace gases and aerosols from biomass burning – an updated](https://doi.org/10.5194/aep-19-8523-2019)
782 [assessment, Atmospheric Chemistry and Physics, 19, 8523–8546, https://doi.org/10.5194/aep-19-](https://doi.org/10.5194/aep-19-8523-2019)
783 [8523-2019, 2019.](https://doi.org/10.5194/aep-19-8523-2019)
- 784 [Aurell, J. and Gullett, B. K.: Emission Factors from Aerial and Ground Measurements of Field](https://doi.org/10.1021/es402101k)
785 [and Laboratory Forest Burns in the Southeastern U.S.: PM_{2.5}, Black and Brown Carbon, VOC,](https://doi.org/10.1021/es402101k)
786 [and PCDD/PCDF, Environ. Sci. Technol., 47, 8443–8452, https://doi.org/10.1021/es402101k,](https://doi.org/10.1021/es402101k)
787 [2013.](https://doi.org/10.1021/es402101k)
- 788 [Aurell, J., Gullett, B., Holder, A., Kiros, F., Mitchell, W., Watts, A., and Ottmar, R.: Wildland fire](https://doi.org/10.1016/j.atmosenv.2021.118193)
789 [emission sampling at Fishlake National Forest, Utah using an unmanned aircraft system,](https://doi.org/10.1016/j.atmosenv.2021.118193)
790 [Atmospheric Environment, 247, 118193, https://doi.org/10.1016/j.atmosenv.2021.118193, 2021.](https://doi.org/10.1016/j.atmosenv.2021.118193)
- 791 [Bian, Q., Ford, B., Pierce, J. R., and Kreidenweis, S. M.: A Decadal Climatology of Chemical,](https://doi.org/10.1029/2019JD031372)
792 [Physical, and Optical Properties of Ambient Smoke in the Western and Southeastern United](https://doi.org/10.1029/2019JD031372)
793 [States, Journal of Geophysical Research: Atmospheres, 125, e2019JD031372,](https://doi.org/10.1029/2019JD031372)
794 [https://doi.org/10.1029/2019JD031372, 2020.](https://doi.org/10.1029/2019JD031372)
- 795 [Binte Shahid, S., Lacey, F. G., Wiedinmyer, C., Yokelson, R. J., and Barsanti, K. C.: NEIVAv1.0: Next-generation Emissions InVentory expansion of Akagi et al. \(2011\) version 1.0, Geoscientific](https://doi.org/10.5194/gmd-17-7679-2024)
796 [Model Development, 17, 7679–7711, https://doi.org/10.5194/gmd-17-7679-2024, 2024.](https://doi.org/10.5194/gmd-17-7679-2024)
- 797 [Bend, T. C., Streets, D. G., Yarber, K. F., Nelson, S. M., Woo, J. H., and Klimont, Z.: A](https://doi.org/10.1029/2003JD003697)
798 [technology-based global inventory of black and organic carbon emissions from combustion,](https://doi.org/10.1029/2003JD003697)
799 [Journal of Geophysical Research: Atmospheres, 109, https://doi.org/10.1029/2003JD003697,](https://doi.org/10.1029/2003JD003697)
800 [2004.](https://doi.org/10.1029/2003JD003697)
- 801 [Bend, T. C., Doherty, S. J., Fahey, D. W., Forster, P. M., Berntsen, T., DeAngelo, B. J., Flanner,](https://doi.org/10.1002/jgrd.50171)
802 [M. G., Ghan, S., Kärcher, B., Koch, D., Kinne, S., Kondo, Y., Quinn, P. K., Sarofim, M. C.,](https://doi.org/10.1002/jgrd.50171)
803 [Sehultz, M. G., Schulz, M., Venkataraman, C., Zhang, H., Zhang, S., Bellouin, N., Guttikunda, S.](https://doi.org/10.1002/jgrd.50171)
804 [K., Hopke, P. K., Jacobson, M. Z., Kaiser, J. W., Klimont, Z., Lohmann, U., Schwarz, J. P.,](https://doi.org/10.1002/jgrd.50171)
805 [Shindell, D., Storelvmo, T., Warren, S. G., and Zender, C. S.: Bounding the role of black carbon](https://doi.org/10.1002/jgrd.50171)
806 [in the climate system: A scientific assessment, Journal of Geophysical Research: Atmospheres,](https://doi.org/10.1002/jgrd.50171)
807 [118, 5380–5552, https://doi.org/10.1002/jgrd.50171, 2013.](https://doi.org/10.1002/jgrd.50171)
- 808 [Burling, I. R., Yokelson, R. J., Akagi, S. K., Urbanski, S. P., Wold, C. E., Griffith, D. W. T.,](https://doi.org/10.5194/aep-11-12197-2011)
809 [Johnson, T. J., Reardon, J., and Weise, D. R.: Airborne and ground based measurements of the](https://doi.org/10.5194/aep-11-12197-2011)
810 [trace gases and particles emitted by prescribed fires in the United States, Atmospheric Chemistry](https://doi.org/10.5194/aep-11-12197-2011)
811 [and Physics, 11, 12197–12216, https://doi.org/10.5194/aep-11-12197-2011, 2011.](https://doi.org/10.5194/aep-11-12197-2011)
- 812 [California Air Resources Board: California's Black Carbon Emission Inventory Technical](https://doi.org/10.1007/978-1-4614-5370-2)
813 [Support Document, 2016.](https://doi.org/10.1007/978-1-4614-5370-2)
- 814 [California Air Resources Board: Greenhouse Gas Emissions of Contemporary Wildfire,](https://doi.org/10.1007/978-1-4614-5370-2)
815 [Prescribed Fire, and Forest Management Activities, California Air Resources Board, Sacramento,](https://doi.org/10.1007/978-1-4614-5370-2)
816 [CA, 2020.](https://doi.org/10.1007/978-1-4614-5370-2)

- 818 Caubel, J. J., Cados, T. E., and Kirchstetter, T. W.: A new black carbon sensor for dense air
819 quality monitoring networks, *Sensors*, 18, 738, <https://doi.org/10.3390/s18030738>, 2018.
- 820 Cazorla, A., Bahadur, R., Suski, K. J., Cahill, J. F., Chand, D., Schmid, B., Ramanathan, V., and
821 Prather, K. A.: Relating aerosol absorption due to soot, organic carbon, and dust to emission
822 sources determined from in-situ chemical measurements, *Atmospheric Chemistry and Physics*,
823 13, 9337–9350, <https://doi.org/10.5194/acp-13-9337-2013>, 2013.
- 824 Chakrabarty, R. K., Shetty, N. J., Thind, A. S., Beeler, P., Sumlin, B. J., Zhang, C., Liu, P.,
825 Idrobo, J. C., Adachi, K., Wagner, N. L., Schwarz, J. P., Ahern, A., Sedlacek, A. J., Lambe, A.,
826 Daube, C., Lyu, M., Liu, C., Herndon, S., Onasch, T. B., and Mishra, R.: Shortwave absorption
827 by wildfire smoke dominated by dark brown carbon, *Nat. Geosci.*, 16, 683–688,
828 <https://doi.org/10.1038/s41561-023-01237-9>, 2023.
- 829 Chelluboyina, G. S., Kapoor, T. S., and Chakrabarty, R. K.: Dark brown carbon from wildfires: a
830 potent snow radiative forcing agent?, *npj Clim Atmos Sci*, 7, 1–10,
831 <https://doi.org/10.1038/s41612-024-00738-7>, 2024.
- 832 Chen, L. W. A., Moesmller, H., Arnott, W. P., Chow, J. C., Watson, J. G., Susott, R. A., Babbitt,
833 R. E., Wold, C. E., Lincoln, E. N., and Hao, W. M.: Emissions from Laboratory Combustion of
834 Wildland Fuels: Emission Factors and Source Profiles, *Environ. Sci. Technol.*, 41, 4317–4325,
835 <https://doi.org/10.1021/es062364i>, 2007.
- 836 Chow, J. C., Watson, J. G., Lowenthal, D. H., Antony Chen, L. W., and Metallebi, N.: PM_{2.5}
837 source profiles for black and organic carbon emission inventories, *Atmospheric Environment*, 45,
838 5407–5414, <https://doi.org/10.1016/j.atmosenv.2011.07.011>, 2011.
- 839 Connolly, R., Marlier, M. E., Garcia Gonzales, D. A., Wilkins, J., Su, J., Bekker, C., Jung, J.,
840 Benilla, E., Burnett, R. T., Zhu, Y., and Jerrett, M.: Mortality attributable to PM_{2.5} from
841 wildland fires in California from 2008 to 2018, *Science Advances*, 10, eadl1252,
842 <https://doi.org/10.1126/sciadv.adl1252>, 2024.
- 843 Cruz Núñez, X., Villers Ruiz, L., and Gay García, C.: Black carbon and organic carbon
844 emissions from wildfires in Mexico, *Atmósfera*, 27, 165–172, [https://doi.org/10.1016/S0187-6236\(14\)71107-5](https://doi.org/10.1016/S0187-6236(14)71107-5), 2014.
- 846 Dong, Q., Meng, X., Gong, J., and Zhu, T.: A review of advances in black carbon exposure
847 assessment and health effects, *CSB*, 69, 703–716, <https://doi.org/10.1360/TB-2023-0409>, 2023.
- 848 El Asmar, R., Li, Z., Tanner, D. J., Hu, Y., O'Neill, S., Huey, L. G., Odman, M. T., and Weber, R.
849 J.: A multi-site passive approach to studying the emissions and evolution of smoke from
850 prescribed fires, *Atmospheric Chemistry and Physics*, 24, 12749–12773,
851 <https://doi.org/10.5194/acp-24-12749-2024>, 2024.

- 852 Feng, Y., Ramanathan, V., and Kotamarthi, V. R.: Brown carbon: a significant atmospheric
853 absorber of solar radiation?, *Atmospheric Chemistry and Physics*, 13, 8607–8621,
854 <https://doi.org/10.5194/acp-13-8607-2013>, 2013.
- 855 Grahame, T. J., Klemm, R., and Schlesinger, R. B.: Public health and components of particulate
856 matter: The changing assessment of black carbon, *Journal of the Air & Waste Management
857 Association*, 64, 620–660, <https://doi.org/10.1080/10962247.2014.912692>, 2014.
- 858 Hadley, O. L. and Kirchstetter, T. W.: Black carbon reduction of snow albedo, *Nature Clim
859 Change*, 2, 437–440, <https://doi.org/10.1038/nclimate1433>, 2012.
- 860 Harrison, R. M., Beddows, D. C. S., Jones, A. M., Calvo, A., Alves, C., and Pio, C.: An
861 evaluation of some issues regarding the use of aethalometers to measure woodsmoke
862 concentrations, *Atmospheric Environment*, 80, 540–548,
863 <https://doi.org/10.1016/j.atmosenv.2013.08.026>, 2013.
- 864 Hosseini, S., Urbanski, S. P., Dixit, P., Qi, L., Burling, I. R., Yokelson, R. J., Johnson, T. J.,
865 Shrivastava, M., Jung, H. S., Weise, D. R., Miller, J. W., and Cocker III, D. R.: Laboratory
866 characterization of PM emissions from combustion of wildland biomass fuels, *Journal of
867 Geophysical Research: Atmospheres*, 118, 9914–9929, <https://doi.org/10.1002/jgrd.50481>, 2013.
- 868 Huang, J., Hopke, P. K., Choi, H. D., Laing, J. R., Cui, H., Zananski, T. J., Chandrasekaran, S.
869 R., Rattigan, O. V., and Holsen, T. M.: Mercury (Hg) emissions from domestic biomass
870 combustion for space heating, *Chemosphere*, 84, 1694–1699,
871 <https://doi.org/10.1016/j.chemosphere.2011.04.078>, 2011.
- 872 Ivančič, M., Gregorič, A., Lavrič, G., Alföldy, B., Ježek, I., Hasheminassab, S., Pakbin, P.,
873 Ahangar, F., Sowlat, M., Boddeker, S., and Rigler, M.: Two-year long high time-resolution
874 apportionment of primary and secondary carbonaceous aerosols in the Los Angeles Basin using
875 an advanced total carbon–black carbon (TC–BC(λ)) method, *Science of The Total Environment*,
876 848, 157606, <https://doi.org/10.1016/j.scitotenv.2022.157606>, 2022.
- 877 Janssen, N. A. H., Hoek, G., Simic-Lawson, M., Fischer, P., van Bree, L., ten Brink, H., Keuken,
878 M., Atkinson, R. W., Anderson, H. R., Brunekreef, B., and Cassee, F. R.: Black carbon as an
879 additional indicator of the adverse health effects of airborne particles compared with PM10 and
880 PM2.5, *Environ Health Perspect*, 119, 1691–1699, <https://doi.org/10.1289/ehp.1003369>, 2011.
- 881 Kaspari, S., McKenzie Skiles, S., Delaney, I., Dixon, D., and Painter, T. H.: Accelerated glacier
882 melt on Snow Dome, Mount Olympus, Washington, USA, due to deposition of black carbon and
883 mineral dust from wildfire, *Journal of Geophysical Research: Atmospheres*, 120, 2793–2807,
884 <https://doi.org/10.1002/2014JD022676>, 2015.
- 885 Keane, R. E. and Lutes, D.: First Order Fire Effects Model (FOFEM), in: *Encyclopedia of
886 Wildfires and Wildland-Urban Interface (WUI) Fires*, edited by: Manzello, S. L., Springer
887 International Publishing, Cham, 1–5, https://doi.org/10.1007/978-3-319-51727-8_74-1, 2018.

- 888 Kirchstetter, T. W. and Thatcher, T. L.: Contribution of organic carbon to wood smoke particulate
889 matter absorption of solar radiation, *Atmospheric Chemistry and Physics*, 12, 6067–6072,
890 <https://doi.org/10.5194/acp-12-6067-2012>, 2012.
- 891 Kirchstetter, T. W., Novakov, T., and Hobbs, P. V.: Evidence that the spectral dependence of light
892 absorption by aerosols is affected by organic carbon, *Journal of Geophysical Research: Atmospheres*, 109, <https://doi.org/10.1029/2004JD004999>, 2004.
- 894 Larkin, N. K., Raffuse, S. M., Huang, S., Pavlovic, N., Lahm, P., and Rao, V.: The
895 Comprehensive Fire Information Reconciled Emissions (CFIRE) inventory: Wildland fire
896 emissions developed for the 2011 and 2014 U.S. National Emissions Inventory, *Journal of the
897 Air & Waste Management Association*, 70, 1165–1185,
898 <https://doi.org/10.1080/10962247.2020.1802365>, 2020.
- 899 BlueSky Modeling Framework: <https://www.airfire.org/data/bluesky>, last access: 12 November
900 2024.
- 901 Laskin, A., Laskin, J., and Nizkorodov, S. A.: Chemistry of Atmospheric Brown Carbon, *Chem. Rev.*, 115, 4335–4382, <https://doi.org/10.1021/cr5006167>, 2015.
- 903 Levinson, R., Akbari, H., and Berdahl, P.: Measuring solar reflectance – Part I: Defining a metric
904 that accurately predicts solar heat gain, *Solar Energy*, 84, 1717–1744,
905 <https://doi.org/10.1016/j.solener.2010.04.018>, 2010.
- 906 Li, J. and Li, Y.: Ozone deterioration over North China plain caused by light absorption of black
907 carbon and organic carbon, *Atmospheric Environment*, 313, 120048,
908 <https://doi.org/10.1016/j.atmosenv.2023.120048>, 2023.
- 909 Liu, C., Chung, C. E., Yin, Y., and Schnaiter, M.: The absorption Ångström exponent of black
910 carbon: from numerical aspects, *Atmospheric Chemistry and Physics*, 18, 6259–6273,
911 <https://doi.org/10.5194/acp-18-6259-2018>, 2018.
- 912 Lutes, D. C.: FOFEM 6.7 User Guide, United States Forest Service, 2020.
- 913 Maji, K. J., Li, Z., Vaidyanathan, A., Hu, Y., Stowell, J. D., Milano, C., Wellenius, G., Kinney,
914 P. L., Russell, A. G., and Odman, M. T.: Estimated Impacts of Prescribed Fires on Air Quality
915 and Premature Deaths in Georgia and Surrounding Areas in the US, 2015–2020, *Environ. Sci.
916 Technol.*, <https://doi.org/10.1021/acs.est.4c00890>, 2024.
- 917 Marsavin, A., Gageldonk, R. van, Bernays, N., May, N. W., Jaffe, D. A., and Fry, J. L.: Optical
918 properties of biomass burning aerosol during the 2021 Oregon fire season: comparison between
919 wild and prescribed fires, *Environ. Sci.: Atmos.*, 3, 608–626,
920 <https://doi.org/10.1039/D2EA00118G>, 2023.
- 921 May, A. A., McMeeking, G. R., Lee, T., Taylor, J. W., Craven, J. S., Burling, I., Sullivan, A. P.,
922 Akagi, S., Collett, J. L., Flynn, M., Coe, H., Urbanski, S. P., Seinfeld, J. H., Yokelson, R. J., and
923 Kreidenweis, S. M.: Aerosol emissions from prescribed fires in the United States: A synthesis of

- 924 laboratory and aircraft measurements, *Journal of Geophysical Research: Atmospheres*, 119,
925 11,826–11,849, <https://doi.org/10.1002/2014JD021848>, 2014.
- 926 McMeeking, G. R., Kreidenweis, S. M., Baker, S., Carriero, C. M., Chow, J. C., Collett, J. L.,
927 Hao, W. M., Holden, A. S., Kirchstetter, T. W., Malm, W. C., Moosmüller, H., Sullivan, A. P., and
928 Wold, C. E.: Emissions of trace gases and aerosols during the open combustion of biomass in the
929 laboratory, *Journal of Geophysical Research: Atmospheres*, 114,
930 <https://doi.org/10.1029/2009JD011836>, 2009.
- 931 Miller, R. K., Field, C. B., and Mach, K. J.: Barriers and enablers for prescribed burns for
932 wildfire management in California, *Nat Sustain.*, 3, 101–109, <https://doi.org/10.1038/s41893-019-0451-7>, 2020.
- 933
- 934 Mek, J., Krotkov, N. A., Arola, A., Torres, O., Jethva, H., Andrade, M., Labow, G., Eck, T. F., Li,
935 Z., Dickerson, R. R., Stenchikov, G. L., Osipov, S., and Ren, X.: Impacts of brown carbon from
936 biomass burning on surface UV and ozone photochemistry in the Amazon Basin, *Sci Rep.*, 6,
937 36940, <https://doi.org/10.1038/srep36940>, 2016.
- 938 Nelson Jr., R. M.: An evaluation of the carbon balance technique for estimating emission factors
939 and fuel consumption in forest fires, *Res. Pap. SE 231*. Asheville, NC: U.S. Department of
940 Agriculture, Forest Service, Southeastern Forest Experiment Station, 231, 9,
941 <https://doi.org/10.2737/SE-RP-231>, 1982.
- 942 North, M., Collins, B., Safford, H., and Stephenson, N.: Montane Forests, in: *Ecosystems of
943 California*, University of California Press, 553–578, 2016.
- 944 Ottmar, R. D.: Wildland fire emissions, carbon, and climate: Modeling fuel consumption, *Forest
945 Ecology and Management*, 317, 41–50, <https://doi.org/10.1016/j.foreco.2013.06.010>, 2014.
- 946 Selimovic, V., Yokelson, R. J., Warneke, C., Roberts, J. M., de Gouw, J., Reardon, J., and
947 Griffith, D. W. T.: Aerosol optical properties and trace gas emissions by PAX and OP-FTIR for
948 laboratory simulated western US wildfires during FIREX, *Atmospheric Chemistry and Physics*,
949 18, 2929–2948, <https://doi.org/10.5194/acp-18-2929-2018>, 2018.
- 950 Stampfer, O., Austin, E., Ganuelas, T., Fiander, T., Seto, E., and Karr, C. J.: Use of low-cost PM
951 monitors and a multi-wavelength aethalometer to characterize PM2.5 in the Yakama Nation
952 reservation, *Atmospheric Environment*, 224, 117292,
953 <https://doi.org/10.1016/j.atmosenv.2020.117292>, 2020.
- 954 Steel, Z. L., Foster, D., Coppoletta, M., Lydersen, J. M., Stephens, S. L., Paudel, A., Markwith,
955 S. H., Merriam, K., and Collins, B. M.: Ecological resilience and vegetation transition in the face
956 of two successive large wildfires, *Journal of Ecology*, 109, 3340–3355,
957 <https://doi.org/10.1111/1365-2745.13764>, 2021.
- 958 Sugrue, R. A., Preble, C. V., Butler, J. D. A., Redon Gabel, A. J., Marconi, P., Shetty, K. D., Hill,
959 L. A. L., Amezeua Smith, A. M., Lukonov, B. R., and Kirchstetter, T. W.: The value of adding

- 960 black carbon to community monitoring of particulate matter, *Atmospheric Environment*, 325,
961 120434, <https://doi.org/10.1016/j.atmosenv.2024.120434>, 2024.
- 962 Tasnia, A., Lara, G., Foster, D., Sengupta, D., Butler, J. D. A., Kirchstetter, T. W., York, R.,
963 Kreisberg, N. M., Goldstein, A. H., Battles, J. J., and Barsanti, K. C.: Comprehensive Fuel and
964 Emissions Measurements Highlight Uncertainties in Smoke Production Using Predictive
965 Modeling Tools, *ACS EST Air*, 2, 982–997, <https://doi.org/10.1021/acs.estair.4c00142>, 2025.
- 966 Thomas, S. C. and Martin, A. R.: Carbon Content of Tree Tissues: A Synthesis, *Forests*, 3, 332–
967 352, <https://doi.org/10.3390/f3020332>, 2012.
- 968 Urbanski, S.: Wildland fire emissions, carbon, and climate: Emission factors, *Forest Ecology and
969 Management*, 317, 51–60, <https://doi.org/10.1016/j.foreco.2013.05.045>, 2014.
- 970 Urbanski, S. P., Hao, W. M., and Baker, S.: Chapter 4 Chemical Composition of Wildland Fire
971 Emissions, in: *Developments in Environmental Science*, vol. 8, edited by: Bytnerowicz, A.,
972 Arbaugh, M. J., Riebau, A. R., and Andersen, C., Elsevier, 79–107,
973 [https://doi.org/10.1016/S1474-8177\(08\)00004-1](https://doi.org/10.1016/S1474-8177(08)00004-1), 2008.
- 974 US Environmental Protection Agency: 2020 National Emissions Inventory Technical Support
975 Document: Fires – Wild, Prescribed, and Agricultural Field Burning, US Environmental
976 Protection Agency, Research Triangle Park, NC, 2023.
- 977 SPECIATE: <https://www.epa.gov/air-emissions-modeling/speciate-0>, last access: 16 January
978 2025.
- 979 Wagstaff, M., Henderson, S. B., McLean, K. E., and Brauer, M.: Development of methods for
980 citizen scientist mapping of residential woodsmoke in small communities, *Journal of
981 Environmental Management*, 311, 114788, <https://doi.org/10.1016/j.jenvman.2022.114788>, 2022.
- 982 Wang, X., Heald, C. L., Sedlacek, A. J., de Sá, S. S., Martin, S. T., Alexander, M. L., Watson, T.
983 B., Aiken, A. C., Springston, S. R., and Artaxo, P.: Deriving brown carbon from multiwavelength
984 absorption measurements: method and application to AERONET and Aethalometer observations,
985 *Atmospheric Chemistry and Physics*, 16, 12733–12752, <https://doi.org/10.5194/acp-16-12733-2016>, 2016.
- 987 Wang, Y., Huang, J., Zananski, T. J., Hopke, P. K., and Holsen, T. M.: Impacts of the Canadian
988 Forest Fires on Atmospheric Mercury and Carbonaceous Particles in Northern New York,
989 *Environ. Sci. Technol.*, 44, 8435–8440, <https://doi.org/10.1021/es1024806>, 2010.
- 990 Wang, Y., Hopke, P. K., Rattigan, O. V., Xia, X., Chalupa, D. C., and Utell, M. J.:
991 Characterization of Residential Wood Combustion Particles Using the Two-Wavelength
992 Aethalometer, *Environ. Sci. Technol.*, 45, 7387–7393, <https://doi.org/10.1021/es2013984>, 2011a.
- 993 Wang, Y., Hopke, P. K., and Utell, M. J.: Urban-scale Spatial-temporal Variability of Black
994 Carbon and Winter Residential Wood Combustion Particles, *Aerosol Air Qual. Res.*, 11, 473–
995 481, <https://doi.org/10.4209/aaqr.2011.01.0005>, 2011b.

- 996 Ward, D. E. and Radke, L. F.: Emissions Measurements from Vegetation Fires: A Comparative
997 Evaluation of Methods and Results, in: *Fire in the Environment: The Ecological, Atmospheric,*
998 *and Climatic Importance of Vegetation Fires*, John Wiley & Sons Ltd., 53–76, 1993.
- 999 Wiedinmyer, C., Quayle, B., Geron, C., Belote, A., McKenzie, D., Zhang, X., O'Neill, S., and
1000 Wynne, K. K.: Estimating emissions from fires in North America for air quality modeling,
1001 *Atmospheric Environment*, 40, 3419–3432, <https://doi.org/10.1016/j.atmosenv.2006.02.010>,
1002 2006.
- 1003 Wu, X., Sverdrup, E., Mastrandrea, M. D., Wara, M. W., and Wager, S.: Low intensity fires
1004 mitigate the risk of high intensity wildfires in California's forests, *Science Advances*, 9,
1005 eadi4123, <https://doi.org/10.1126/sciadv.ad4123>, 2023.
- 1006 Yang, S., Xu, B., Cao, J., Zender, C. S., and Wang, M.: Climate effect of black carbon aerosol in
1007 a Tibetan Plateau glacier, *Atmospheric Environment*, 111, 71–78,
1008 <https://doi.org/10.1016/j.atmosenv.2015.03.016>, 2015.
- 1009 Yokelson, R. J., Burling, I. R., Gilman, J. B., Warneke, C., Stockwell, C. E., de Gouw, J., Akagi,
1010 S. K., Urbanski, S. P., Veres, P., Roberts, J. M., Kuster, W. C., Reardon, J., Griffith, D. W. T.,
1011 Johnson, T. J., Hosseini, S., Miller, J. W., Coker III, D. R., Jung, H., and Weise, D. R.: Coupling
1012 field and laboratory measurements to estimate the emission factors of identified and unidentified
1013 trace gases for prescribed fires, *Atmospheric Chemistry and Physics*, 13, 89–116,
1014 <https://doi.org/10.5194/acp-13-89-2013>, 2013.
- 1015 Zeng, L., Dibb, J., Scheuer, E., Katich, J. M., Schwarz, J. P., Bourgeois, I., Peischl, J., Ryerson,
1016 T., Warneke, C., Perring, A. E., Diskin, G. S., DiGangi, J. P., Nowak, J. B., Moore, R. H.,
1017 Wiggins, E. B., Pagonis, D., Guo, H., Campuzano-Jost, P., Jimenez, J. L., Xu, L., and Weber, R.
1018 J.: Characteristics and evolution of brown carbon in western United States wildfires,
1019 *Atmospheric Chemistry and Physics*, 22, 8009–8036, <https://doi.org/10.5194/acp-22-8009-2022>,
1020 2022.
- 1021 Zhang, A., Wang, Y., Zhang, Y., Weber, R. J., Song, Y., Ke, Z., and Zou, Y.: Modeling the global
1022 radiative effect of brown carbon: a potentially larger heating source in the tropical free
1023 troposphere than black carbon, *Atmospheric Chemistry and Physics*, 20, 1901–1920,
1024 <https://doi.org/10.5194/acp-20-1901-2020>, 2020.
- 1025